RECOMMENDATIONS FOR

Seismic Design of Hybrid Coupled Wall Systems

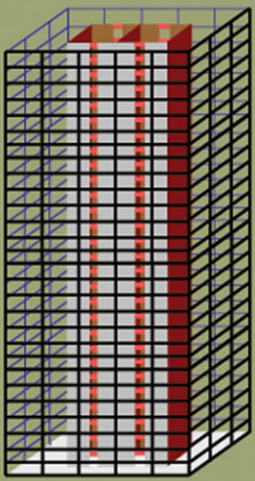

EDITED BY

Sherif El-Tawil
Patrick Fortney
Kent Harries
Bahram Shahrooz
Yahya Kurama
Mohammad Hassan
Xiangdong Tong

ASCE

SEI
Structural Engineering Institute

RECOMMENDATIONS FOR SEISMIC DESIGN OF HYBRID COUPLED WALL SYSTEMS

PREPARED BY
Technical Committee on Composite Construction
The Structural Engineering Institute (SEI)
of the American Society of Civil Engineers

EDITED BY
Sherif El-Tawil
Patrick Fortney
Kent Harries
Bahram Shahrooz
Yahya Kurama
Mohammad Hassan
Xiangdong Tong

Published by the American Society of Civil Engineers

Library of Congress Cataloging-in-Publication Data

Recommendations for seismic design of hybrid coupled wall systems / prepared by ASCE Technical Committee on Composite Construction ; edited by Sherif El-Tawil … [et al.].
p. cm.
Includes bibliographical references and index.
ISBN 978-0-7844-1060-8
1. Concrete walls--Design and construction. 2. Reinforced concrete construction--Design and construction. 3. Earthquake resistant design. I. El-Tawil, Sherif. II. ASCE Technical Committee on Composite Construction.

TH2245.R43 2009
693.8'52--dc22 2009025848

American Society of Civil Engineers
1801 Alexander Bell Drive
Reston, Virginia, 20191-4400

www.pubs.asce.org

ISBN 978-0-7844-1060-8
Manufactured in the United States of America.

Acknowledgments

This document was prepared by a task group working under the auspices of the Technical Committee on Composition Construction of the Structural Engineering Institute (SEI) of the American Society of Civil Engineers (ASCE). Funding for this effort was provided through an ASCE SEI Special Project. The task group appreciates the encouragement and advice provided by the ASCE SEI Technical Administrative Committee on Metals and the ASCE SEI Technical Activities Division Executive Committee. The authors also wish to acknowledge the contributions, over the years, of their graduate students who have worked on aspects of research reported in these Recommendations. The opinions in this report are those of the authors and do not necessarily represent the views of the American Society of Civil Engineers.

This page intentionally left blank

Contents

List of Figures

List of Tables

List of Variables

A	Sum of the areas of the individual wall piers ($A = A_1 + A_2$)
A_b	gross area of the coupling beam
A_g	Gross area of a wall
A_s	Area of tension reinforcement
A_{sel}	Cross-sectional area of longitudinal wall reinforcement provided over embedment length, L_e
A_s'	Area of compression reinforcement
A_{tb}	Area of transfer bar reinforcement in one region of embedment, top and bottom of beam
A_v	Area of stirrup reinforcement within spacing s in composite coupling beam
b_f	Coupling beam flange width
b_w	Coupling beam web thickness
b_{wC}	Composite coupling beam thickness (total thickness)
c	Concrete cover (assumed to spall)
C_d	Deflection amplification factor
C_f and C_b	Concrete bearing forces
CR	Coupling ratio
d	Wall effective section depth as defined by ACI-318
d_C	Composite coupling beam depth (total depth)
DL	Dead load component
E	Young's modulus
f_c'	Concrete compressive strength
f_{yr}	Nominal yield strength of stirrup reinforcement in composite coupling beam
g	Effective clear span given by Equations 2 or 3
g_{clear}	Clear span between two adjacent walls
G	Shear Modulus
h	Story height
H_1	Resultant height of the fundamental mode inertial force distribution
I	sum of the moments of inertia of the individual wall piers ($I = I_1 + I_2$)
I_b	Gross moment of inertia of the coupling beam
I_c	Moment of inertia of the coupling beam accounting for shear deformations
I_g	Gross moment of inertia of a wall
L	Lever arm between the centroids of the wall piers

LL	Live load component
L_b	Length of coupling beam
L_e	Embedded coupling beam length
L_w, l_w	Web length of a concrete wall
m_w, m_{eff}, $m_{eff,2}$	Total mass, effective fundamental mode mass, and effective second mode mass
m_i	Overturning moment resisted by wall *i*
M_{wu}	Maximum base moment strength of the coupled wall structure
N	Number of stories
OTM	Overturning moment
P	Pier axial force computed using Equations 11 and 13
PGA	Peak acceleration of the ground motion
$Q_{w,max}$	Maximum base shear demand
$Q_{1,max}$	Fundamental mode component of base shear demand
$Q_{h,max}$	Higher mode component of base shear demand
R	Response modification coefficient
R_y	Ratio of the expected yield stress to the specified minimum yield stress
s	Spacing of stirrups or reinforcement
t_w	Web thickness of a concrete wall
$V_{beam,i}$	Coupling beam shear at level *i*.
V_e	Expected shear capacity of a coupling beam
V_f	Coupling beam shear design force determined from factored lateral loading
V_n	Nominal shear capacity of a coupling beam
Ω_o	Overstrength factor
γ	Wall overstrength factor
δ_H	Wall drift ratio computed for the highest point on the wall
θ_d	Interstory drift angle
θ_b	Coupling beam rotation
β_1	Ratio of the average concrete compressive strength to the maximum stress
ε_f and ε_b	Concrete strains in Figure 15
λ	Shape factor

1 Introduction

Reinforced concrete (RC) coupled wall systems, where RC beams couple two or more RC walls in series are frequently used in medium and high-rise construction. The benefits of coupling in such systems are well recognized and understood. The coupling beams provide transfer of vertical forces between adjacent walls, which creates a frame-like coupling action that resists a portion of the total overturning moment induced by the seismic action. This coupling action has three major beneficial effects. First, it reduces the moments that must be resisted by the individual wall piers resulting in a more efficient structural system. Secondly, it provides a means by which seismic energy is dissipated over the entire height of the wall system as the coupling beams undergo inelastic deformations. A final important advantage of a coupled wall system is that it has a lateral stiffness that is significantly greater than the sum of its component wall piers, permitting a reduced footprint for the lateral load resisting system.

The structural response of coupled walls is, however, complicated by the fact that the system is comprised of components that exhibit significantly different ductility demands. Figure 1 shows the idealized lateral force-deformation response of a coupled wall structure as the sum of the individual cantilever pier flexural responses and the frame-like response of the coupling action provided by the beams. In contrast to the walls, the coupling beams must undergo significant inelastic deformations in order to allow the structure to achieve its lateral yield strength, R_T. As the system continues to deform laterally in a ductile manner, the wall ductility ratio, defined as the ratio of the ultimate deformation to that at yield, is significantly smaller than that of the beams. If the beams are unable to cope with the high ductility demands imposed upon them, the coupling action deteriorates, leading to a drop in the lateral resistance and a dramatic change in the dynamic properties as the system eventually degenerates into two (or multiple) independent, uncoupled wall piers.

The shear force and deformation demands expected on coupling beams during a design-level seismic event, coupled with their low span-to-depth ratio and the degradation of shear resisting mechanisms attributed to concrete under load reversals, have led designers to provide special diagonal reinforcement detailing for and in the vicinity of RC coupling beams (ACI 2008). This special reinforcement complicates erection, potentially increasing both construction time and cost. Furthermore, the limited shear capacity of RC coupling beams often requires designers to provide impractically deep members (Harries et al. 2005). To mitigate these problems, some engineers have turned to structural steel coupling beams as an alternative to reinforced concrete beams. The resulting structural system is referred to as a hybrid coupled wall (HCW) system and is the subject of this report.

Hybrid coupled wall systems are often built in conjunction with steel framing systems. For example, Figure 2a shows a building with a HCW core (Figure 2b) and a perimeter steel frame. The combined structural system may be considered to be a dual frame-wall system. For most practical designs, however, the high stiffness of the

coupled core wall system exceeds the influence of the more flexible steel frame. The wall system will therefore attract the majority of the earthquake-induced lateral loads and must be designed accordingly.

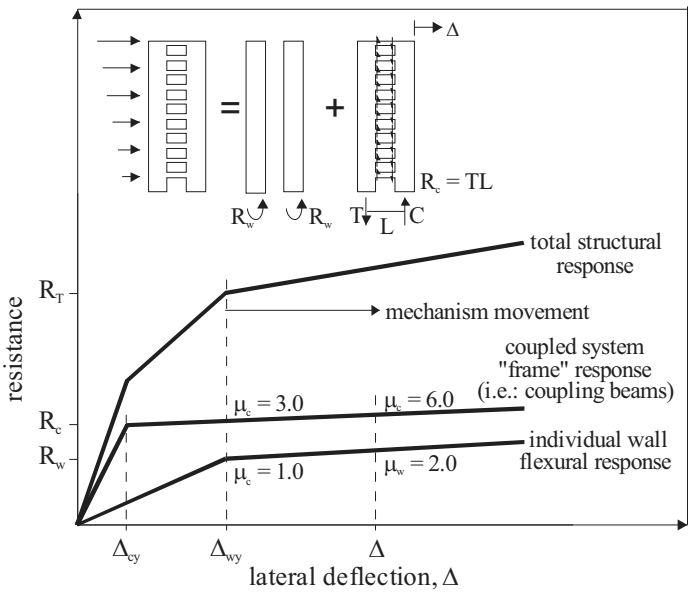

Figure 1: Idealized lateral response of coupled wall structure

In response to seismic excitation, steel coupling beams are expected to dissipate energy in a manner that is similar to the response of shear links in eccentrically braced frames. Shear links, and coupling beams in turn, fall into three categories: short, intermediate, and long, depending on their structural and geometric properties (AISC Seismic 2005). When architectural constraints permit, short coupling beams which dissipate energy primarily through inelastic shear distortion are preferred to longer coupling beams that dissipate energy through flexural hinge rotation. Mechanisms that involve inelastic shear deformation in steel coupling beams are generally more ductile than those involving flexure-related plastic hinge deformations.

The detailing of beam-to-wall connections depends on whether steel columns are embedded in the wall boundaries. Relatively light steel frame members are sometimes used in hybrid steel-concrete construction for erection purposes or as wall boundary element reinforcement. If steel column boundary elements are used, the coupling beams can frame into the columns and transmit the coupling forces through a moment resisting connection with the steel column (Figure 3a). Such a structural system may

include a horizontal steel framing member within the wall spanning between boundary elements to facilitate transfer of the coupling beam moments through the depth of the wall (Taranath 1998), although such an element is not strictly required (AISC Seismic 2005). The provision of a moment connection is, however, not preferred given the cost and difficulty of constructing ductile connections that must deliver performance similar to or, in many cases, exceeding that of connections in special moment resisting steel frames (as specified, for example, in AISC Seismic 2005). Alternatively, the embedded coupling beam may be connected to the embedded column with a shear connection while the moment resistance is provided by a combination of the embedment length and shear transfer afforded by headed studs along the beam flanges in combination with special reinforcement detailing in the wall boundary region This detail, shown in Figure 3(b), was used in First City Tower, Houston (Taranath 1998). It is more typical, however, not to use boundary steel columns and to embed the coupling beams a sufficient distance into the wall so that the coupling forces can be transmitted entirely through the interaction that occurs between the embedded beam and the wall as shown in the detail in Figure 4 corresponding to the wall system shown in Figure 2(b)[1].

A small number of buildings with HCW lateral load resisting systems have been constructed in regions of moderate to high seismicity. Harries and Shahrooz (2005) list examples of these buildings, the earliest of which was constructed in the mid-1960s in New Zealand. In spite of the necessity for interaction and coordination between trades during construction, site reports from the contractors erecting the buildings suggest few construction challenges. None of the buildings constructed to date have experienced a major earthquake, and so there is limited field information about their performance under strong seismic shaking.

HCW systems have been studied both experimentally and analytically since the 1960's. In the US, research on HCW systems was conducted under the auspices of the US-Japan Program on Composite and Hybrid Structures funded by the US National Science Foundation. Key conclusions from completed US and Canadian studies can be summarized as follows (Deason et al. 2001; El-Tawil et al. 2003, 2002a,b; Fortney et al. 2007a,b; Fortney et al. 2006a; Fortney 2005; Gong and Shahrooz 2001a,b,c; Gong et al. 1998; Harries et al. 2000, 1998, 1996, and 1992, Hassan and El-Tawil 2004, Rassati et al. 2006, Shahrooz et al. 2004a,b, 2001, 1993, 1992; Xuan and Shahrooz 2005): i) HCW systems possess the necessary combination of stiffness, strength, and toughness for adequate performance in regions of moderate to high seismicity; ii) they are economical compared to pure reinforced concrete shear wall systems; and iii) it is feasible to develop performance-based design guidelines for such systems.

[1] It is interesting to note that although the original detail, shown in Figure 4, prescribes cross ties passing through the coupling beam web, this detail was abandoned in the actual construction (Figure 2(b)) in favor of using hooked ties on either side of the web and a short vertical bar between the flanges to anchor the ties (Lehmkuhl 2002).

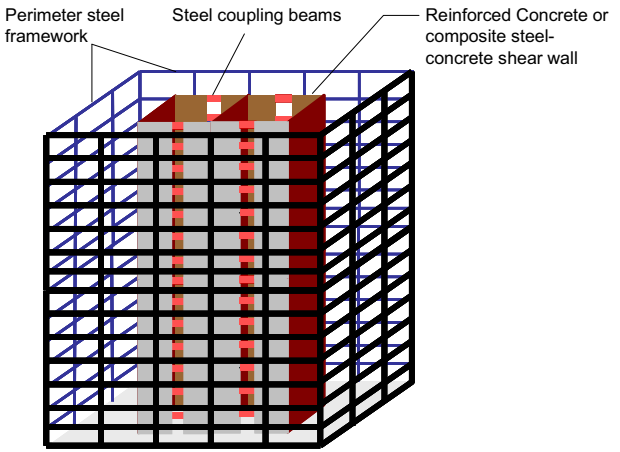

(a) Schematic representation

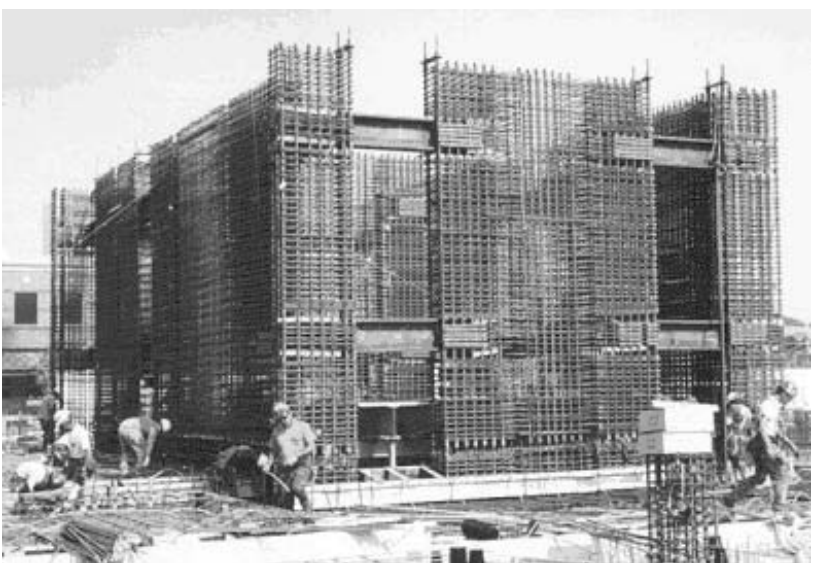

(b) HCW core under construction*

Figure 2: Building with HCW core and steel perimeter frame
* *Courtesy of Mr. Eric Lehmkuhl, printed with permission*

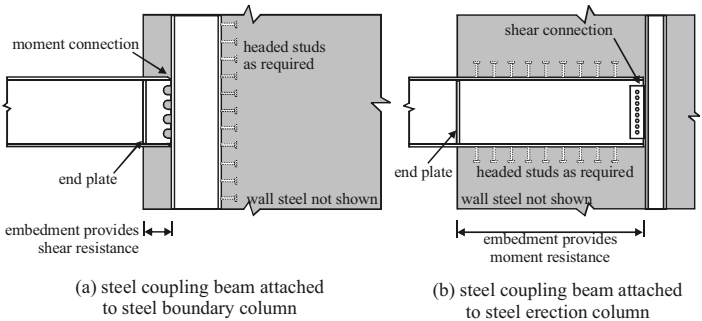

Figure 3: Two types of connections between coupling beams and embedded steel columns.

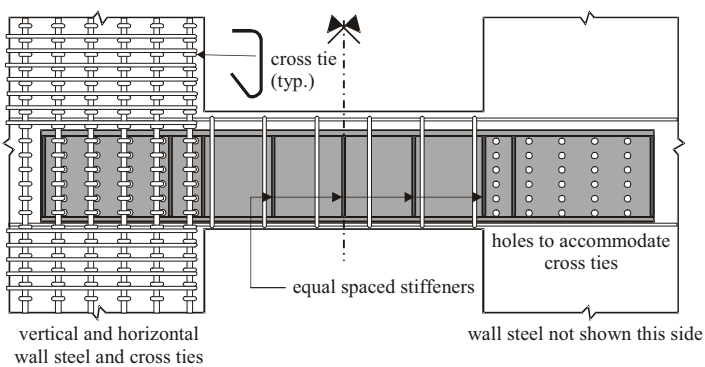

Figure 4: Example of typical detail of coupling beam embedded in RC wall (adapted from Lehmkuhl 2002). See footnote 1 on page 11 for additional information.

After approximately four decades of construction history and about fifteen years of extensive experimental and computational research activity, existing design guidelines for HCW systems are still quite limited. The main design specifications that address this system are prescriptive provisions published within the AISC Seismic Provisions for Structural Steel Buildings (2005). These provisions trace their origin to the 1994 NEHRP provisions (BSSC 1994), which introduced general provisions for composite steel-concrete structures. The 1994 NEHRP provisions for hybrid walls were adopted with some changes into a new section of the 1997 AISC Seismic provisions called: Part II - Composite Structural Steel and Reinforced Concrete Buildings. The same provisions were included by reference in the 1997 NEHRP Recommended Provisions (BSSC 1997) and the International Building Code (ICC 2000). Design provisions for HCW have not been substantially changed in

successive editions of the AISC Seismic Provisions, where they still reside. Furthermore, there has been no coordinated effort to develop performance-based design provisions that are specific to HCW and comparable to those proposed for steel systems (e.g. FEMA-350 2000) or other types of systems including reinforced concrete systems, e.g. FEMA 273 (1997) and its successor document FEMA-356 (2000).

Even though HCW systems have documented and well understood structural and economic benefits compared to alternative traditional systems, they continue to be used with reluctance in practice, mostly in situations where designers have little alternative. Part of the reason for this is the lack of well established design guidelines that designers can refer to when considering the system. The objective of this report is to synthesize existing information into practical recommendations that can be utilized by practitioners in the design of HCW systems in regions of moderate to high seismic risk.

1.1 Application

The recommendations made in this document are for proportioning HCW systems comprised of two or more reinforced concrete walls connected with steel beams distributed along the height of the walls. Only beam-to-wall connections where moment is transferred by embedment of the steel section into the wall (Figure 4) are considered. The recommendations can be applied to design the lateral load resisting system and its components including structural walls, coupling beams, and the connections between the beams and walls.

The provisions in this document are based largely on research conducted by Deason et al. (2001), El-Tawil et al. (2003, 2002a,b), Fortney et al. 2007a,b, Fortney et al. (2006), Fortney (2005), Gong and Shahrooz (2001a,b,c), Gong et al. (1998), Harries et al. (2000, 1998, 1996, and 1992), Hassan and El-Tawil (2004), Rassati et al. (2006), Shahrooz et al. (2004a,b, 2001, 1993, 1992), and Xuan and Shahrooz (2005). Where applicable, the recommendations also draw upon existing specifications for steel and concrete, as well as other research on composite systems.

1.2 Scope

The recommendations have been derived from limited test data and computational results. Therefore, they should not be applied to configurations that are substantially different than those considered in the development of these provisions. The provisions apply for proportioning systems with the following characteristics:

- Material specifications: normal weight concrete, with concrete strength not exceeding 70 MPa; reinforcing steel bars with specified yield strength not less than 280 MPa and not greater than 410 MPa; and A36, A572 Gr. 50, or A992 structural steel (specified yield strength of 345 MPa). These limits are imposed due to lack of experimental data for connections with light weight or high strength concrete or steels with higher strengths.

- Geometric specifications: The core wall thickness in the connection region must be equal to or wider than the width of the steel coupling beam (i.e., the steel beam must fit inside curtains of wall steel and/concentrated reinforcement in the wall end boundary element).
- System layout: The provisions are suitable for horizontally and vertically regular systems comprised of two or more wall piers coupled in series.
- Beam-Wall connection types: The provisions are suitable for embedded connections where steel beams are embedded into the wall piers as described in Chapter 5 and shown in Figures 4 and 14.
- Application: the provisions can be applied to buildings in regions of moderate to high seismicity.

2 System Behavior, Analysis, and Design Considerations

Research over the past half century on coupled wall systems has shown that their structural performance is strongly influenced by the amount of coupling provided by the system. Although the majority of studies have focused on reinforced concrete coupled wall systems, the system behavior and mechanics are the same for all coupled wall structures including hybrid systems. Indeed, the behavior itself is a manifestation of the classic dowelled cantilever problem described by Chitty (1947).

Figure 5 shows a coupled wall system deformed under the influence of lateral loads, which cause a global system overturning moment, *OTM*. In response to the applied loading, a coupling beam, *j*, develops end moments (not shown in the figure) and corresponding shears, $V_{beam,j}$, which act on the individual walls as shown in Figure 5. The coupling beam shear forces push down on one wall and pull up on the other. The coupled system resists *OTM* through the development of an axial force couple ($\Sigma V_{beam,j}$ over the lever arm L), resulting from the accumulation of the effect of beam shears, as well as flexural reactions in the individual wall piers, (m_1 and m_2) as shown in Figure 5. Base shear is resisted by shear reactions at the bases of the wall piers. The proportion of *OTM* resisted by the couple is defined as the Coupling Ratio (*CR*).

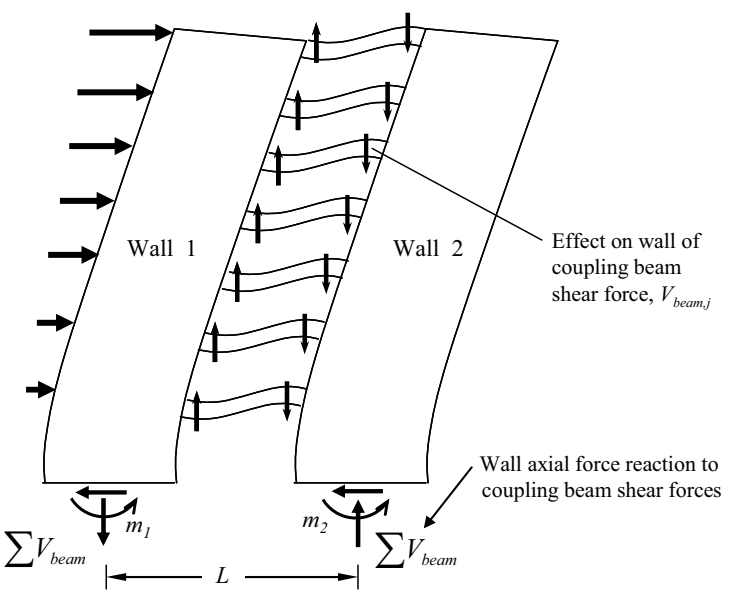

Figure 5: Definition of the coupling ratio (CR)

For a two-wall system, the coupling ratio is defined as:

$$CR = \frac{L\sum V_{beam}}{L\sum V_{beam} + \sum m_i} = \frac{L\sum V_{beam}}{OTM} \quad (1)$$

Where $\sum V_{beam}$ is the accumulation of coupling beam shears acting at the edge of one wall pier; L is the lever arm between the centroids of the wall piers and m_i is the overturning moment resisted by wall i. To gain insight into the meaning of this ratio, consider the following cases: i) CR=0 implies that coupling beams develop no end moments (the beams are not present or are pinned links) and therefore there is no coupling action whatsoever; ii) CR=50% implies that the coupling action resists half the imposed overturning moments, while the remaining half of the resistance to the OTM is provided by individual wall pier moment reactions (m_1 and m_2 in Figure 5); and iii) CR=100% is the theoretical case where the two wall piers effectively behave as a single pier which may be envisioned as the case where the beam length approaches zero.

By convention, the calculation of CR is made at the base of the wall when the system forms a mechanism. In this idealized case, the coupling beams are assumed to maintain their plastic shear capacity as the wall piers yield. This definition is adopted herein.

As noted previously, coupled structures are significantly stiffer than the sum of their component wall piers. Figure 6 provides an illustration of the beneficial effects of coupling two identical wall piers having uniform coupling beams over their height and subjected to an inverse triangular loading (Harries et al. 2004a). In this figure, the roof deflection determined from an elastic analysis, normalized to that of a pair of uncoupled (connected with a pinned link) wall piers, is plotted against CR. The increased structural stiffness, even at modest values of CR, is apparent.

As indicated earlier, the CR is traditionally defined at the base of the wall. The coupling ratio also varies as the walls deform under loading due to the spread of inelasticity and higher mode effects. Figure 7 shows how the CR (determined at the base of the structure) changes as the lateral pushover load increases in a lightly coupled 12-story prototype HCW system. As the lateral load increases from zero, the system initially responds elastically. As cracking in the wall piers initiates and spreads through the system, the CR increases with increasing lateral load level to a maximum of about 27%. This peak coincides with the initiation of yielding in the coupling beams. The contribution from coupling starts to drop as the relative contribution from the cracked walls continues to increase. The CR is minimized when both walls yield at their bases. After the minimum point, the CR rises slowly again because the coupling beams harden at a faster rate than the walls do.

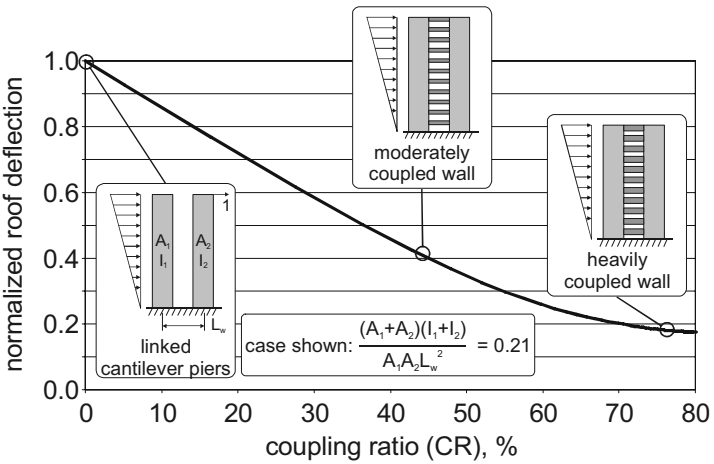

Figure 6: Effect of coupling on wall pier roof displacement (adapted from Harries et al. 2004a)

The summation of coupling beam shear forces ($\sum V_{beam}$) implies that the reinforced concrete wall piers to which the beams are attached are subjected to axial forces – in addition to gravity loads – that vary during an earthquake as a result of the coupling action. It is therefore possible for the net compressive axial force acting on a wall to increase substantially, which can reduce the ductility of the wall and induce premature crushing failure (El-Tawil et al. 2002b; Aktan and Bertero 1984). Similarly, the net load acting on a wall may decrease substantially or reverse direction subjecting the wall to axial tension, which also adversely influences the shear capacity of the wall and impacts the design of the foundation system. Finally, these axial stress reversals, themselves, may cause considerable degradation of wall pier behavior. Thus, wall pier axial-moment-shear (PMV) interaction behavior is an important parameter in the design and accurate analyses of HCW systems.

Research reported by El-Tawil et al. (2002b) on 12-story coupled wall systems quantifies the effects of the *CR*. Systems with high coupling (*CR* = 60%) had more widespread cracking in the upper portions of the wall piers and suffered earlier crushing failure of the walls compared to systems with lower coupling ratios. At the other extreme, no coupling at all (CR = 0%) can also lead to inefficient and comparatively poor behavior. For example, of all the prototypes considered in the research, the system without any coupling experienced the highest base wall rotations, story drifts, shear distortions and deflections, in addition to experiencing concrete crushing in the plastic hinge region. Systems with coupling ratios of 30% to 45% performed best amongst the systems considered and were most economical in the sense that they required less steel and concrete materials. Figure 8 shows how the amount of concrete and steel materials required for design varied with the amount of designed-for system coupling.

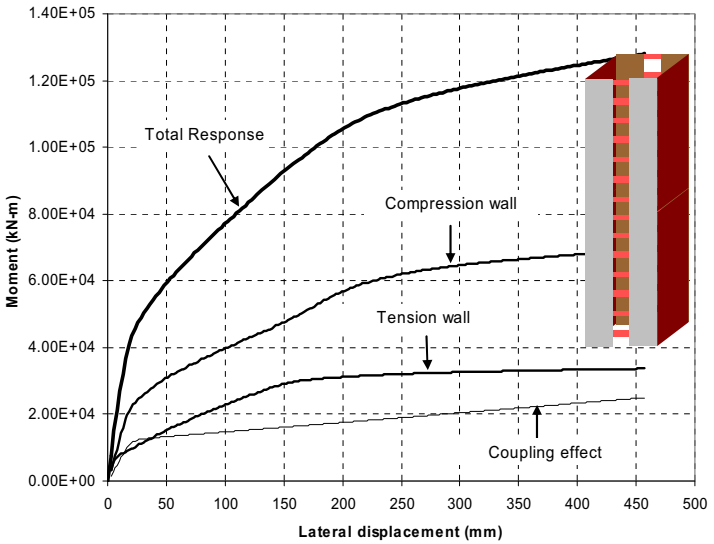

(a) Moment versus displacement responses of individual system components

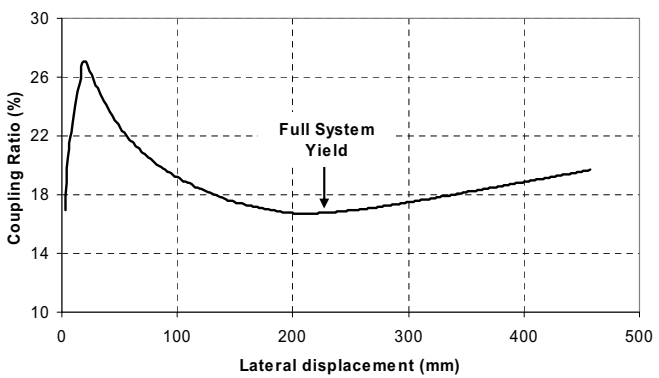

(b) Coupling ratio versus displacement level

Figure 7: Pushover of hybrid coupled wall structure showing change in *CR*

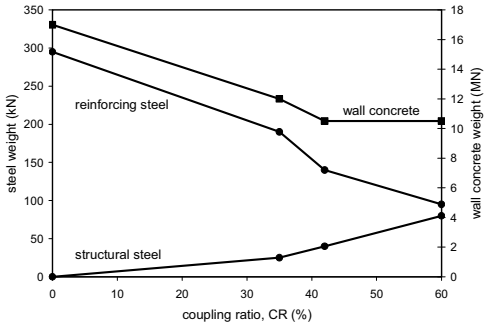

Figure 8: Steel and concrete weight as a function of *CR* for a 12 story HCW prototype building (El-Tawil et al. 2002a)

It is noted that in their research, El-Tawil et al. (2002b) assumed uniform coupling beam details over the height of the 12-story structures considered. Harries and McNiece (2006), in a study of reinforced concrete coupled walls, found that making such an assumption in substantially taller buildings (30 stories) could adversely affect the behavior of the wall piers in the upper regions of the structure where higher mode responses become significant.

Harries and McNiece (2006) recommend "grouping" coupling beams and allowing for vertical redistribution of coupling beam forces (similar to that allowed in the Canadian A23.3 Concrete Design Standard (CSA 2004)) in order to minimize demands on the wall piers while continuing to provide coupling action consistent with the expected behavior of the system. Xuan and Shahrooz (2005) also recommend grouping coupling beams based on the distribution of coupling beam shear demand over the building height. This concept is discussed in Section 3.4. Examples of structures having grouped coupling beams over the height of the structure are shown in Figure 9. Figure 9(b) also illustrates the tapering of the wall pier stiffness over the height of a tall structure.

2.1 Selection of Coupling Ratio

The choice of a suitable coupling ratio (*CR*) depends greatly on the judgment and experience of the designer. Certainly, there is little structural benefit to providing a low *CR* as the reduction in wall moments and lateral drifts will be relatively inconsequential. An example of a low *CR* that is generally not considered in design is the small level of coupling offered simply by the presence of a slab coupling the wall piers (Lim 1989). Generally the slab is assumed to provide no resistance to lateral forces, although the slab-to-wall connections must be detailed to have the necessary ductility to satisfy compatibility requirements.

On the other hand, it has been shown that a high *CR* results in inordinately large ductility demands on reinforced concrete coupling beams (Harries 2001). A high *CR* implies reduced moment demands on the wall piers, allowing smaller wall sections.

However, the high *CR* also results in a greater axial couple, resulting in a greater likelihood that the walls will experience net tension and uplift. Similarly, the high axial compression forces that result may substantially reduce the ductility of wall members. These combined effects indicate that a high *CR* may result in an impractical design scenario.

While Harries (2001) proposed a practical upper limit of 66% for the *CR* of HCWs, El-Tawil et al. (2002b) recommend that the *CR* range from 30% to 45% for an efficient design. This latter recommendation is based on a study of 12-story HCW buildings with uniform coupling beams over the height of the building (Figure 9a).

Applying a performance-based design approach, Harries and McNiece (2006) designed two 30-story reinforced concrete structures having *CR* values of 67% and 78%. In these designs, five coupling beam details were distributed over the height of the structure and the wall capacities were reduced three times over the wall height (Figure 9b). Xuan et al (2007) designed an efficient reinforced concrete 15-story structure using three groups of coupling beams having the largest capacities in the lower one half of the wall height (Figure 9c). The resulting *CR* for this structure was approximately 80%. In a case where uniform wall and concrete beam details were provided, Harries et al. (2004b) demonstrate the design of a ten-story structure having a *CR* of 74%.

Although a design exhibiting good behavior and satisfying all performance criteria was obtained in each case discussed above, the designs would not be strictly compliant with current building code requirements for strength-based design. Using a conventional strength-based design methodology, the *CR* must be reduced to approximately 50% to result in a "designable" structure and often lower to ensure compliance with strength-based code provisions, thus illustrating some of the restrictions of conventional or diagonally reinforced concrete coupling beams. These latter observations agree well with the recommendations of El-Tawil et al. (2002b) and conclusions drawn by Aktan and Bertero (1984) from their earlier analytical and experimental studies.

Whereas conventionally and diagonally reinforced concrete coupling beams have a number of code-prescribed and practical constructability limitations (Harries et al. 2005), the use of steel coupling beams and thus HCWs overcome many of these. In particular, the use of built-up sections effectively eliminates limitation on beam shear capacity and thus the selection of the CR.

The foregoing discussion indicates that various researchers have successfully utilized a wide range of coupling ratios. Based on published works, it appears that there is little structural advantage to providing a CR less than about 30%. Similarly, an upper limit to ensure sound structural performance is in the range of 60% to 80%. With HCWs, this upper limit, unlike CCWs where the CR upper limit is controlled by beam shear limitations, is largely based on controlling the wall pier axial load developed as a result of the coupling action which, combined with the factored

gravity load acting on the compression pier, should not overload the wall pier in compression.

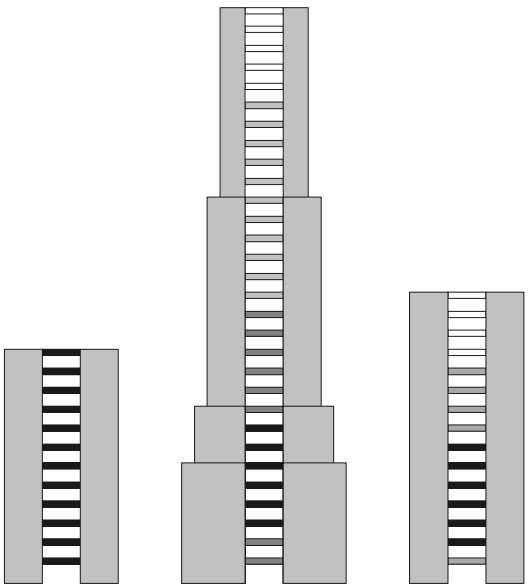

(a) El-Tawil et al. (2002b) (b) Harries and McNeice (2006) (c) Xuan and Shahrooz (2007)

Figure 9: Schematic representation of wall and beam capacity distribution and resulting CR
(beam capacity proportional to degree of shading.)

Although ACI-318 Chapter 21 (2008) does not enforce a limit, FEMA-356 (2000) – based on SEAOC (1999) – prohibits walls having gravity-induced axial compression loads greater than 35% of the wall axial capacity from contributing to lateral resistance of the structure. FEMA-356 (2000) also limits the deformation capacity of walls based upon the amount of axial load and shear present. According to this specification, a wall having an axial load less than 10% of the wall's axial capacity has the greatest permitted flexural ductility – 0.015 radians of plastic hinge rotation for the collapse prevention performance level when there is low shear (defined as $V < 3\sqrt{f_c'}t_w l_w$) and a confined boundary element. In contrast, walls having axial loads greater than 25% of the wall's axial capacity have the smallest permitted flexural ductility: 0.009 radians of plastic hinge rotation for the collapse prevention performance level when there is low shear and a confined boundary element. FEMA-

356 (2000) recommends that walls with an axial load greater than 35% of the walls' axial capacity not be counted upon for lateral resistance; the implication is that such walls cannot deliver ductile performance. Based on these arguments, it is therefore recommended that a wall pier in a HCW not have a net axial compression load greater than 35% of its compressive capacity. A review (Fortney et al. 2008) of a number of concrete and hybrid coupled wall designs presented in available literature (Harries and McNeice 2006, Harries et al. 2004b, Xuan et al. 2007) reveals maximum wall pier compression forces in the vicinity of 20% of the walls' gross axial capacity at the ultimate limit state.

2.2 Analysis Models for HCWs

Several types of linear and nonlinear analysis models have been used to model shear walls. These models fall into three main classes: i) equivalent frame models; ii) multi-spring models; and, iii) continuum finite element models. Figure 10 shows examples of these models.

In the equivalent frame model, the finite width of the walls is generally represented using rigid elements, while wall behavior is modeled using an equivalent beam-column element placed at the wall centroid. In these models, the cross-sectional response is represented by resultant or fiber section models (as shown in Figure 10a). In multi spring models, the behavior of the wall is represented using a number of series/parallel springs to simulate the inelastic axial, shear, and bending behavior of the wall panels, while rigid elements are used to represent the physical dimension of the wall. Examples of beam-column and multi-spring models can be found in Otani (1980), Charney (1991), Colotti (1993), Kunnath et al. (1992), Cheng et al. (1993), Shahrooz et al. (1993), Harries et al. (1998 and 2004b), Harries and McNiece (2006) and), and Fortney et al. (2007b). Continuum finite element analyses of reinforced concrete wall systems are reported in Bolander and Wight (1991), Chesi and Schnobrich (1991), Sittipunt and Wood (1995), and El-Tawil et al. (2002a, b).

Until about a decade ago, *elastic* equivalent frame and multi-spring representations (Figure 10a, b) were preferred by practicing structural engineers because they could be conveniently implemented and run on then-existing commercial analysis software. Finite element models were generally shunned because: i) the software required for conducting analysis was expensive, specialized and required specialized knowledge; and ii) finite element analysis produces stresses, which must then be integrated (usually manually) to obtain the forces required for structural design. Advances in structural analysis software have addressed both limitations, and structural engineers now routinely use *elastic* finite element models (Figure 10c) to analyze structural walls, particularly flanged walls and walls with irregular geometry.

At present, nonlinear finite element analysis modeling tools remain limited in their abilities and must be operated by knowledgeable and competent analysts to produce reasonable and trustworthy results. In contrast, nonlinear beam-column analysis models (both resultant and fiber section models) are becoming increasingly available and reliable. Since it is unlikely that nonlinear finite element analysis will be used in

the design office, beam-column models are recommended for routine design and nonlinear analysis of hybrid coupled walls. It should be noted, however, that since the location of the wall neutral axis changes substantially during a nonlinear analysis, beam-column elements (which are generally placed at the wall centroids) can be grossly inaccurate unless they adequately account for the effects of axial-flexural interaction. For this reason, fiber-section models are recommended to capture the wall pier behavior. Special attention should be paid to ensure that shear behavior is either adequately considered in the model or that its effect can be conservatively ignored. Following are more detailed modeling guidelines.

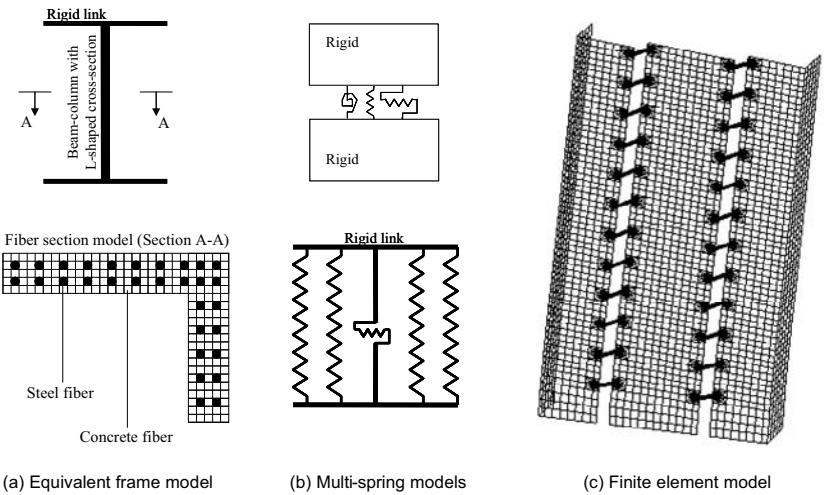

Figure 10: Methods for modeling shear walls in HCWs.

2.2.1 Equivalent Frame Models

The beam-column element formulation used in an equivalent frame analysis of a HCW system should satisfy a number of constraints:

- *For linear analyses:* the elements used should account for the flexural as well as shear stiffness of both wall and coupling beam members. Guidance on choosing member stiffness is provided in Section 3.2.
- *For nonlinear analysis:* the elements should accurately represent flexural and shear stiffnesses and strengths as well as the deformation capacities of the members. Additionally, the elements must have well defined axial-moment (P-M) interaction relationships and must be capable of taking the effect of this interaction into account. The models must also represent the behavior of unsymmetric wall shapes that have different stiffness, strength and deformation

capacity in different directions (i.e., unsymmetric P–M interaction relationships). For nonlinear cyclic models, the models must also represent the deterioration of strength and stiffness that occurs with load reversals.

Spacone and El-Tawil (2004) surveyed the techniques commonly used to represent cross-section response of equivalent frame models. Of the techniques used, two methods are commonly used to model cross-sectional behavior: section resultant models and fiber section models.

Resultant models explicitly define section responses in terms of moment-curvature, axial load-axial strain, etc. The simplest resultant models decouple flexural and axial responses, with each following linear or nonlinear relationships such as the Takeda et al. (1970) model relating section moment and curvature. Such models are not recommended for the analysis of HCWs. More advanced resultant models that consider axial-flexure interaction include the models by Hilmy and Abel (1985), Hajjar and Gourley (1997) and El-Tawil and Deierlein (2001). Such models are more appropriate for the analysis of HCWs.

In a fiber section model, the section is subdivided into a number of fibers (not necessarily of equal area) and the stresses are integrated over the cross-sectional area to obtain stress resultants such as force or moment. The fiber section model generally makes use of a number of assumptions: i) Plane sections remain plane in bending. It is generally accepted that this assumption is reasonably accurate even well into the inelastic range; ii) Shear and torsion stresses are neglected[1]. For this reason, the fiber method is generally used for the analysis of flexure dominated members, where Euler-Bernoulli beam theory can be reasonably applied; iii) Although constitutive relations are typically defined as uniaxial, multi-axial stress states (such as those due to confinement effects) can be included by increasing the concrete strength and/or by modifying the concrete post-peak response; iv) Concrete cracking is taken into account. However, the cracking is considered to be smeared and normal to the member axis as a result of the plane section assumption; v) Local buckling of the steel components and initial stresses resulting from either erection loads or thermal residual effects can be included. Each fiber in the section can be assigned concrete, structural steel, or reinforcing bar material properties. Making use of the "plane sections remain plane" assumption and from relevant constitutive models, fiber stresses are calculated from the fiber strains. Examples of fiber models can be found in Kurama (2002) and Kurama et al. (2002).

In a hybrid approach, fiber-section analyses (such as those which may be accomplished using RESPONSE (Bentz 2000) or XTRACT (Imbsen 2004)) are used to develop axial force-moment (PM) or axial force-moment-shear (PMV) interaction relationships which are then applied to simpler equivalent frame beam-column representations of the wall piers. This approach minimizes model complexity while overcoming some of the issues associated with simplification. Examples of this

[1]commercial software packages are available that include shear degradation models in their treatment of P-M interaction for concrete elements. (e.g., PERFORM 3D (formerly RAM PERFORM)).

approach are presented by Harries and McNeice (2006), Harries et al. (2004b), Fortney et al. (2007b), and Xuan et al. (2007). It should be noted that the hybrid approach has the same model limitations as the equivalent frame approach since the changes that occur in the location of the wall neutral axis during a nonlinear analysis cannot be represented.

For flanged walls, the effective flange width must be determined for the sectional analysis. The flange width is specified by ACI-318 Section 21.9.5.2 for both tension and compression flanges. However, as discussed in Hassan and El-Tawil (2003), two key factors affect the accuracy of the ACI-318 recommendations for the effective width for flanges in tension: the level of axial force on wall and the drift level. Another issue with the ACI provisions is that the effective width is tied to wall height and not wall length. The results presented by Hassan and El-Tawil (2003) and others based on work on T-beams (e.g. Pantazopoulou and Moehle 1991) suggest that wall length is a more significant parameter. Although a calibration based on wall height is certainly reasonable and acceptable if wall length is proportional to wall height, in many cases such a predetermined relationship between height and length cannot be assumed. Coupled walls are good examples of situations where wall width may not have a typical relationship to wall height because the efficiency of the system allows engineers to design individual wall piers with aspect ratios that are significantly greater than equivalent isolated walls. The criteria in Table 1 (Hassan and El-Tawil 2003) could be used for determining the effective width for flanges in tension as a function of applied load and expected system drift level. Interpolation can be used to obtain values for intermediate conditions. The compression flange width can be computed from the ACI-318 recommendations as the smaller of one half the distance to the adjacent wall web and 25% of the wall height (ACI 2008).

Application of these recommendations is practically difficult for reversed cyclic analysis because the wall piers alternate between tension and compression and can have varying deformation demands during a dynamic analysis. In this case, it is recommended that the tension effective width for the highest expected drift level be utilized for both compression and tension walls.

Table 1: Effective Width for Wall Flanges in Tension

Loading Case	**System Drift Level**		
	0.5%	1%	2%
Walls Subjected to Tension or Pure Flexure	*d*	1.5*d*	2*d*
When the compression force in the wall is > $0.05 f_c' A_g$	0.5*d*	0.75*d*	*d*

d is the effective section depth per ACI-318 (2008).

Figure 11 shows a model that is suitable for representing the behavior of HCWs. The model features beam-column elements for the coupling beams and walls. A rigid link is used to represent the physical size of the walls, and a rigid connection is assumed between the coupling beam and the rigid link.

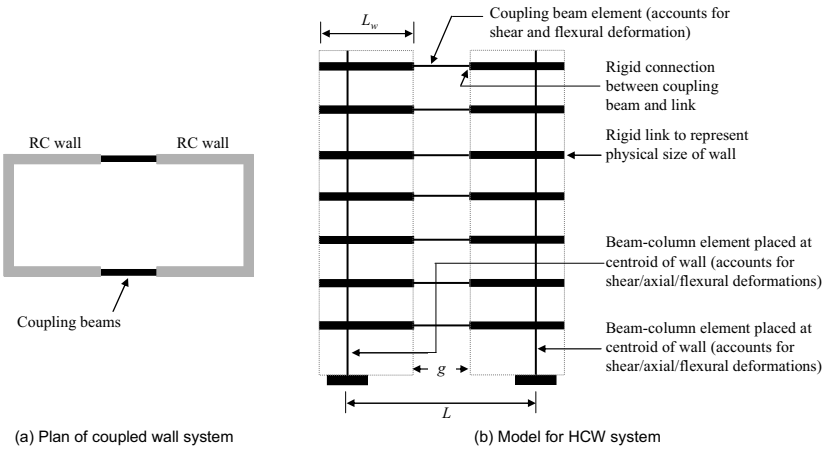

Figure 11: Model for HCW

2.2.2 Finite Element Models

Finite element models used to analyze a HCW system should be constructed with the following points in mind. In general, plane stress membrane elements or shell elements are suitable for modeling wall components. Solid element models should be used when detailed 3-D internal stress and strain distributions are needed.

- *For linear analyses:* The effective Young's modulus should be reduced to account for the expected effect of cracking.
- *For nonlinear analysis:* The analysis model should account for the nonlinear behavior of concrete under tension, compression and multiaxial conditions. Elements modeling steel reinforcement and components should be able to yield under uniaxial and multiaxial states of stresses. If deemed important, sliding shear behavior along construction joints, bond slip between steel bars and surrounding concrete, shear or bond-slip behavior along lapped splices or anchorages, instability of thin walled sections, and bar buckling of the longitudinal compression steel should also be modeled. Nonlinear models of this sort are sensitive to input parameters and can have mesh directivity and element size sensitivity issues. Therefore, it is recommended that nonlinear finite element models should only be used by knowledgeable and competent analysts. In addition, any developed models should be thoroughly validated prior to use by comparing their results to accepted benchmark results and/or to existing test data.

2.3 System Design Philosophy

The preferred yielding mechanism for coupled walls is that the coupling beams yield first over the entire height of the structure followed by yielding at the bases of the wall piers (Paulay and Santhakumar 1976). Energy dissipation from the coupling

beams, prior to the walls yielding reduces the amount of damage resulting from moderate earthquakes by limiting the relatively large displacements associated with wall pier hinging. In order for this energy dissipation to occur, the coupling beams must be sufficiently strong and stiff and behave in a ductile manner, exhibiting a large and stable hysteretic response through the anticipated deformations. To achieve this target performance, two design methods are presented in Chapters 3 and 4: the Prescriptive Design Method (PrDM) and the Performance Based Design Method (PBDM), respectively.

3 Prescriptive Design Method (PrDM)

The prescriptive design method is based on a linear elastic analysis of the structure. Both the Equivalent Lateral Force Analysis (ELFA) and the Modal Response Spectrum Analysis (MRSA) methods are suitable for prescriptive design of HCW systems. Linear Response History Analysis (LRHA), on the other hand, is not recommended because linear, dynamic models are not able to adequately represent the responses of "tension" and "compression" piers, which change substantially when the loading reverses direction. For example, reversal in the direction of lateral loading on a pier requires that its effective structural properties (*EA* and *EI*) be changed as discussed in the following section. The limits of applicability of both ELFA and MRSA are defined in Table 4.4-1 in FEMA-450 (2003).

3.1 Classification According to Current Provisions

For seismic applications, systems with HCW are classified as Special Composite Reinforced Concrete Shear Walls with Steel Elements in FEMA-450 (2003). The design values reported in Table 4.3-1 of FEMA-450 (2003) are applicable, i.e. $R = 6$, $C_d = 5$, and $\Omega_o = 2.5$. If the HCW system acts in conjunction with a moment resisting frame to resist lateral loads, the building is considered to have a dual system. In this case, the total seismic force resistance is provided by the combination of the moment frame and the HCW system in proportion to their rigidities. Given the high stiffness of the walls compared to the frames, most of the lateral seismic loads will be resisted by the HCW system. The frame must nonetheless be proportioned to resist 25% of the lateral loads and must be detailed as a special moment frame so that it can "go along for the ride". In this case, the design values for the system are $R = 7$, $C_d = 6$, and $\Omega_o = 2.5$.

3.2 System Analysis

In order to compute the elastic distribution of internal forces and deformations under the influence of code specified lateral forces, it is important to accurately model the wall pier, coupling beam elements and the connections between them.

3.2.1 Wall Model

Recommendations for reduced section properties, accounting for cracking and loss of stiffness due to cycling of concrete walls vary. Table 2 shows the reduced stiffness values suggested by the current ACI (2008), CSA (2000) and NZS (1995) standards. It is interesting to note that using the reduction factors recommended by the New Zealand Standard, one computes effectively stiffer coupling beams and more flexible wall piers, leading to greater beam forces, and hence a larger coupling ratio, than one computes with the ACI or Canadian recommendations.

Harries et al. (2004a,b and 2005) propose that the following *average* cracked stiffnesses be assigned to the wall piers; these values are consistent with ACI 318 practice:

- walls in the assumed hinge region: $0.35EI_g$ and $0.75EA_g$

- walls above the hinge region expected to remain essentially elastic: $0.70EI_g$ and $1.00EA_g$

Harries et al. further recommended that the flexural stiffness in the hinge regions of the tension and compression walls be balanced to result in an average stiffness *no greater than* $0.35EI_g$.

The effective flexural stiffnesses of the compression and tension walls may be determined from any rational analysis method, including fiber section analysis. Programs such as RESPONSE (Bentz 2000) or XTRACT (Imbsen 2004) are suitable in this regard. Design iterations may be necessary to determine the appropriate level of axial load that should be used in the section analyses.

Table 2: Currently recommended reduced member stiffnesses for wall elements.

Member	ACI 318	CSA A23.3	NZS 3101[1]
compression wall in flexure	$0.70EI_g$	$0.80EI_g$	$0.45EI_g$
tension wall in flexure	$0.35EI_g$	$0.50EI_g$	$0.25EI_g$
compression wall axial	$1.00EA_g$	$1.00EA_g$[2]	$0.80EA_g$
tension wall axial	$0.35EA_g$ (inferred)	$0.50EA_g$[2]	$0.50EA_g$

1. *NZS 3101* has different recommendations for different limit states. The values corresponding to the most critical limit state are shown.
2. *CSA A23.3* suggests that an average axial wall stiffness is appropriate to simplify analyses.

3.2.2 Coupling Beam Model

The coupling beams should be modeled using elements that account for both flexural and shear properties of the beam.

3.2.3 Beam-Wall Connection Model

Previous studies (Shahrooz et al. 1993; Gong et al. 1998; Harries et al. 1997) observed that steel or steel-concrete composite coupling beams are not effectively "fixed" at the face of the wall. The additional flexibility needs to be taken into account to ensure that wall forces and lateral deflections are computed with reasonable accuracy. Based on experimental data (Shahrooz et al. 1993; Gong et al. 1998), the "effective fixed point" of steel or steel-concrete composite coupling beams may be taken at approximately one-third of the embedment length from the face of the wall. Thus, the effective clear span, g, of the frame element representing the coupling beam in the model shown in Figure 11 is:

$$g = g_{clear} + 0.6L_e \tag{2}$$

Equation 2 assumes that the walls have been modeled by beam-column elements located at the centroids of wall piers as shown in Figure 11b and that the shear and flexural properties of the steel coupling beam member are taken into account.

During the preliminary design stage, the embedded coupling beam length, L_e in Equation 2, is still unknown. The procedure proposed by Harries et al. (1997) has

been shown to be effective for taking into account the additional flexibility associated with the beam embedment for beams having a variety of embedment details. In this procedure, the effective stiffness (including both shear and flexural components) of a steel coupling beam is reduced to 60% of its original value. The effective length of the beam is increased by the wall cover dimension, *c*, to account for expected spalling at the face of the wall:

$$g = g_{clear} + 2c \tag{3}$$

Both Equations 2 and 3 assume that the embedment of the coupling beam into the wall provides the necessary moment resistance at the beam end. For steel or steel-concrete composite coupling beams connected to a vertical steel member embedded in the wall boundary region (as shown in Figure 3a), the effective clear span should be taken as the distance between the faces of the embedded vertical "columns".

3.3 Vertical Redistribution of Coupling Beam Forces

Permitting vertical redistribution of coupling beam forces in design can make the design more efficient (Harries and McNeice 2006). Redistribution can also help to lower the required wall overstrength and improves constructibility by permitting engineers to use one beam section over larger vertical portions of the wall. Canadian practice (CSA 2004) permits up to 20% vertical redistribution of shear forces between beams provided the sum of the resulting beam shear capacities exceeds the sum of the factored beam shears (i.e., $\sum V_n / \sum V_f \geq 1$) as shown in Figure 12.

Given the benefits of redistribution and the inherent ductility of steel coupling beams, a 20% redistribution of coupling beam design forces is recommended as long as the aggregate shear capacity of all of the coupling beams exceeds the total coupling shear demand computed over the height of the entire wall.

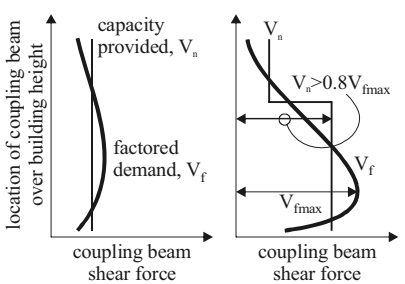

(a) low *CR* (b) high *CR*

Figure 12: Vertical distribution of coupling beam shear

3.4 Beam and Wall Overstrength

In order to ensure the preferred plastic mechanism in RC coupled wall systems, i.e., that the coupling beams yield prior to the wall piers, some existing codes require that the walls must be stronger than the beams that frame into them (CSA 2004; NZS

1995). To achieve this behavior, a wall overstrength factor, γ, is applied to the wall design forces. The required wall overstrength is taken as the ratio of the sum of the nominal shear capacities of the coupling beams, V_n, magnified by $1.1R_y$, to the sum of the coupling beam shear design forces determined for the case of factored lateral loading, V_f, (excluding the effects of torsion) (CSA 2004):

$$\gamma = \sum 1.1R_y V_n \Big/ \sum V_f \tag{4}$$

This factor, therefore, includes the natural overstrength resulting from the design procedure and strength reduction factors and the overstrength resulting from designing for critical beams and using this design over a vertical cluster of beams (or all the beams) in the structure.

The required wall overstrength can have a significant effect on wall pier design forces (Fortney et al. 2007b; Harries and McNeice 2006) and can adversely affect the economy of the system. Required wall overstrength will typically be greater in structures having a higher coupling ratio due to the relatively steep gradient of beam shear demand over the height of the structure (Figure 12; also discussed in Appendix I and shown in Figure I.2). An advantage of a greater coupling ratio is that wall pier forces are reduced, but the larger wall overstrength factor may negate this advantage. This effect may be minimized by permitting the redistribution of beam forces as described in the previous section.

3.5 Design Process

The recommended design process using the PrDM is as follows:

1. Assume preliminary member sizes based on architectural constraints and experience. Alternatively, the preliminary proportioning method specified in Section 4.4 may be used.
2. Construct a linear elastic model according to recommendations in Sections 2.2 and 3.2.
3. Assign preliminary member structural properties according to information in Section 3.2.
4. Apply ELFA or MRSA procedures according to Section 3.1 to obtain member design forces and global deformations.
5. Redistribute coupling beam shear forces according to Section 3.3.
6. Calculate the wall overstrength factor as described in Section 3.4 and apply it to the wall design forces.
7. Apply design provisions outlined in Chapter 5 to ensure that chosen member sizes are sufficient and detail the structural members.
8. Ensure that the force acting on the compression pier due to factored gravity loads plus the sum of the sum of the coupling beam nominal shear capacities magnified by $1.1R_y$ does not exceed 35% of the axial capacity of the wall as described in Section 2.1.

9. Once member proportions have been chosen and system considerations satisfied, check displacement limits according to the ELFA or MRSA procedures described in Section 3.1.
10. Iterate until a design that satisfies both strength and displacement limits are achieved.
11. If a steel frame is used in conjunction with the wall, proportion the frame according to provisions in Section 3.1 and AISC-Seismic (2005).

4 Performance-Based Design Method (PBDM)

A viable and attractive alternative to PrDM is the performance-based design method (PBDM). Performance-based design allows the designer to select how the structure will behave and provides the framework for selecting performance objectives for the structure. Performance objectives are typically displacement-based or force-based objectives; however, they can address any aspect of building performance. For instance, for reinforced concrete coupled walls, a key performance objective is to have a beam that is reasonably constructible (Harries et al. 2004; Harries and McNiece 2006; Xuan et al. 2007).

FEMA-273 (1997) is the first formalized US document to describe methods and design criteria that can be used by engineers to conduct performance-based seismic evaluation. The guidelines in FEMA-273 are comprised of three basic components: i) Definition of a performance objective, categorized in the guidelines by three primary performance levels: Immediate Occupancy (IO), Life Safety (LS) and Collapse Prevention (CP); ii) Demand prediction using four alternative analysis procedures; and iii) Acceptance criteria using force and/or deformation limits which are intended to satisfy the desired performance objective. To encourage wider acceptance of the concepts in FEMA-273, FEMA-356 (2000) which attempts to describe the performance-based approach in "code language" was subsequently released.

The provisions in FEMA-356 (2000) were developed for performance-evaluation of existing structures for the purposes of assessing the need for rehabilitation. The provisions are, however, considered to be conceptually applicable to new buildings as well. In a typical design situation, each design iteration can be considered to represent an existing building whose potential performance is evaluated through the provisions in FEMA-356. As such, the performance-based design provisions recommended herein are modeled after and draw upon provisions in FEMA-356. Because FEMA 356 focuses on existing structures, its reported acceptance criteria may be conservative in some cases when applied to well-detailed new construction. It is expected that future performance-based design criteria that are developed specifically for new buildings will have the same basic elements of FEMA-356, i.e., specification of performance objectives, demand prediction, and acceptance criteria. This is likely true even if future provisions are not deterministic, but rather probabilistic in nature; such as FEMA-350 (2000). The current recommendations are written with this consideration in mind and are in a format that can be conveniently modified as new performance-based design frameworks are proposed.

4.1 Performance Objectives

In most building code applications, the desired performance of a structure is that it will satisfy Life Safety (LS) requirements at the design level earthquake (conventionally defined as having a 10% probability of exceedance in 50 years (10/50)) and Collapse Prevention (CP) requirements at the maximum credible event (2% in 50 years (2/50)). A third performance objective, Immediate Occupancy (IO); associated with a frequent but mild event, i.e. an earthquake with a probability of

exceedance of 50% in 50 year (50/50 earthquake) is also considered in this document. These three performance objectives are therefore recommended for hybrid coupled walls (Harries and McNeice 2006; Hull and Harries 2008).

4.2 Recommended Analysis Methods

The analysis procedures recommended in FEMA-356 (2000) are Linear Static (Equivalent Lateral Force Analysis, ELFA), Nonlinear Static (Pushover), Linear Dynamic, and Nonlinear Dynamic. The choice of analytical method is subject to limitations based on building characteristics. The linear procedures assume linear component and system behavior, but incorporate adjustments to global response parameters to account for the possibility of nonlinear system behavior during the design seismic event.

Of the two nonlinear procedures permitted, the dynamic procedure requires considerable judgment and experience on the part of the user, and therefore has significant limitations on its use – not the least of which is requiring a third-party peer review of the analysis and resulting design. The nonlinear static procedure - also known as a pushover analysis - employs simplified nonlinear techniques to quantify seismic behavior. Pushover analyses have become popular because they avoid the complexity of a nonlinear response history analysis yet incorporate significant aspects of system degradation that are critical to seismic behavior. However, the pushover method, as described in FEMA-356, does not directly account for the presence of higher modes, particularly critical in taller buildings, and is therefore limited to low to mid-rise buildings whose behavior is dominated by first mode response. In this method, a nonlinear model of the building in question is displaced to a target displacement under the action of monotonically increasing lateral loads. The target displacement is intended to represent the maximum displacement likely to be encountered during the design earthquake and is dependent on the chosen level of seismic risk and the dynamic properties of the structure.

The load patterns commonly used in pushover analysis are invariant and are based on the initial elastic dynamic properties of the structure. Changes in the modal attributes of the structure during inelastic seismic response are therefore not accounted for (Kalkan and Kunnath 2006). Several researchers have proposed enhanced pushover procedures to account for higher mode effects while retaining the simplicity of invariant load patterns. These procedures use a variety of modal combination techniques, e.g.: i) a single pushover analysis where the load vectors reflect the contributions from each elastic mode-shape considered (Jan et al. 2003); ii) multiple pushover analyses using invariant load patterns based on elastic mode shapes where the contribution from each mode is combined at the end (Chopra and Goel 2002); iii) analyses wherein the inelastic response obtained from first-mode pushover analysis is combined with the elastic contribution of higher modes (Chopra et al. 2004); and, iv) factored modal combinations (Kunnath 2004).

In the search for more accurate pushover procedures, a number of researchers have made use of adaptive load patterns where changes in the modal attributes of the

structure are accounted for during inelastic behavior. For example, Gupta and Kunnath (2000) proposed an adaptive pushover procedure based on an elastic demand spectrum. In this procedure, a conventional response spectrum analysis is used to derive the load pattern during each pushover step. Several other pushover procedures based on adaptive load patterns have also been proposed (Elnashai 2000; Antoniou et al. 2000; Antoniou and Pinho 2004; Kalkan and Kunnath 2006). All these enhanced "pushover" procedures have been shown to provide improved estimates of interstory drift values compared to conventional nonlinear-static-procedures (NSPs) that utilize inverted triangular, uniform or other lateral load patterns based on direct modal combination rules suggested in FEMA-356 (2000). It should be noted that FEMA-356 (2000) permits the use of adaptive pushover procedures, but does not give guidance on how to setup or utilize the procedure.

Of the permitted procedures, Linear Static, Modal Analysis, Nonlinear Static and Nonlinear Dynamic procedures are recommended for application to hybrid walls. However, preference is given to nonlinear procedures over linear procedures.

4.3 Modeling Guidance

The guidance given in Section 2.2 should be used in conjunction with modeling information and limitations in FEMA-356 to construct suitable linear and nonlinear models for hybrid walls. The following considerations should be taken into account.

- The effects of horizontal torsion should be considered in accordance with FEMA-356 Section 3.2.2.2.
- Diaphragms should be considered in accordance with FEMA-356 Section 3.2.4.
- P-Delta effects should either be explicitly accounted for in the model through a large displacement, small strain formulation or through the provisions of FEMA-356 Section 3.2.5.
- Soil-structure interaction effects should be considered through the provisions of FEMA-356 Section 3.2.6.
- Concurrent seismic effects should be accounted for through the provision of FEMA-356 Section 3.2.7.
- Overturning effects should be investigated in accordance with FEMA-356 Section 3.2.10.

4.3.1 Load Model

The dead and live loads in both nonlinear models should be taken as specified in ASCE 7 (2005). When the gravity and earthquake load effects are additive, the gravity load is determined as $1.2DL + 0.5LL$[1].When the gravity and earthquake load effects counteract one another, the gravity loads should be taken as $0.9DL$ (no live load).

[1] $1.2DL + 1.0LL$ when $LL_0 > 100$ psf

The earthquake and gravity effects should not be obtained from separate models and combined because superposition is not valid for nonlinear analysis. Unless it can be determined by inspection that one case or the other controls behavior, it is recommended that 2 separate analyses be conducted, one for each load case (FEMA-273 1997).

4.3.2 Component Force-Deformation Response for Nonlinear Analysis Procedures

The coupling beam and wall force deformation responses need to be specified when either of the nonlinear analysis methods is employed for performance evaluation. In defining these relationships, it is recommended that both wall and coupling beam strengths be based on the nominal, and *not* the expected, yield strength of the material.

This recommendation stems from the need to ensure that the wall moments are not substantially underestimated when coupling beam overstrength is accounted for. The potentially detrimental effect of coupling beam overstrength is indirectly recognized when the acceptance criteria are investigated in Section 4.5.

4.3.3 Simplified Model for Nonlinear Static Procedure

In lieu of a more detailed model for the Nonlinear Static (Pushover) Procedure, the following recommendations can be used. The backbone curve parameters defined in FEMA-356 Table 5-6 can be used to model the steel coupling beams. Similarly, the backbone curve parameters defined in FEMA-356 Table 6-18 can be used to model the RC wall hinge region. The force P in the RC wall equations should be calculated as follows.

For the Compression Pier: Add the factored gravity load to the summation of the nominal shear capacities of the coupling beams. That is:

$$P = 1.2DL + 0.5LL + \left|\Sigma V_n\right| \quad [1] \tag{5}$$

For the Tension Pier: Add the factored gravity load to the summation of the nominal shear capacities of the coupling beams. That is:

$$P = 0.9DL - \left|\Sigma V_n\right| \tag{6}$$

4.4 Preliminary Proportioning

Since the coupling ratio is a fundamental design parameter that significantly influences the economy and seismic performance of the system, it is important that the designer have control over it. The PrDM in which "elastic" properties are initially assumed followed by design iterations until the design is finalized will force the designer to accept whatever *CR* results from this process. Additionally, this process is sensitive to the selection of cracked section properties. Subtly different stiffness

[1] $P = 1.2DL + 1.0LL + \Sigma V_n$ when $LL_0 > 100$ psf

assumptions can result in significantly varying *CR*s and design loads (Harries et al. 2004a).

In PrDM, the primary means by which to achieve substantially different coupling ratios is to modify the clear span of the coupling beams or change their geometry (depth, width) in an attempt to change the stiffness properties and hence force demands in the elastic system. The former is usually not feasible because of architectural constraints. The latter approach, while feasible for systems with reinforced concrete coupling beams where cracked section properties for the beam can be assumed, is not viable for systems with steel coupling beams. Furthermore, not only are the design iterations time consuming, but also the resulting *CR* is governed by assumed "elastic" properties of the system and may be greater or smaller (depending on the properties of the coupling beams) than that actually experienced by the system under the design seismic event. This may lead to an inaccurate estimate of force demands within the system.

The PBDM framework permits the designer to control the system *CR* to achieve good economy and structural performance simultaneously. Within this framework, the designer can propose any structural configuration and then verify that the resulting system meets the required performance objectives. If not, design iterations are conducted until the required solution is achieved. The key is to choose a preliminary design that minimizes the number of iterations. The following is a recommended method for selecting preliminary HCW parameters.

4.4.1 Method of Determining Trial Proportioning for HCWs

The following HCW system proportioning method, which allows the designer to specify a target *CR*, can be used within the PBDM philosophy to provide an initial design (El-Tawil et al 2002a). An advantage of the method is that it does not require inelastic analysis. The method assumes that the system deforms primarily in its first mode as a result of formation of plastic hinges at the base of the shear walls and simultaneous yielding of all coupling beams along the building height. This is generally a reasonable assumption for low to mid-rise buildings. Analysis results presented in Hassan and El-Tawil (2005) suggest that this assumption is reasonable for the 12- and 18-story buildings that they considered. For taller buildings, whose response is affected by higher vibration modes, the proposed design method will be conservative because not all the beams are likely to yield at the same time.

Step 1 – Select a desired target coupling ratio, CR. (Section 2.1). If the dimensions of the wall piers are established (e.g. as a result of architectural specification), proceed directly to the next step. Otherwise the deflection-based method in Section I.4, Appendix I, may be used to select preliminary system dimensions.

Step 2 – Determine the system base overturning moment (OTM) from the code-prescribed equivalent lateral force analysis (ELFA).

Step 3 – Calculate the overturning couple (sum of coupling beam forces) using the value of *CR* selected in Step 1, the OTM found in Step 2 and the known value of *L*, the distance between wall centroids, and N, the number of stories. Rearranging Equation 1:

$$\sum_{i=1}^{N} V_{beam,i} = \frac{CR.OTM}{L} \tag{7}$$

Step 4 – Distribute coupling beam shears vertically. The total shear force established in Step 3 is distributed to the coupling beams to obtain the design shear force for each beam. If all the coupling beams have the same design, then the shear carried at each beam is simply:

$$\sum_{i=1}^{N} V_{beam,i} \Big/ N \tag{8}$$

This is recommended for structures that do not have significant[1] higher mode effects.

For taller structures, it is recommended that coupling beam design be changed every few stories in a manner consistent with the performance demands of the system. In such cases, it is suggested that the distribution of coupling beam resistance roughly follow that computed from an elastic analysis. Coupling beam distribution for the case of an inverted triangular load and varying coupling ratios are given by Equation I.11 and examples are shown in Figure I.2. In Figure I.2 the horizontal axis (offset for clarity) gives the individual beam shear as a proportion of the sum of the beam shears calculated in Equation 7. These curves can be used to calculate the shear attributed to each beam. The basis for the calculation of these curves is provided in Appendix I.

Vertical redistribution of beam forces is permitted provided the sum of the beam shear capacity exceeds ΣV_{beam} calculated in Equation 7. Redistribution on the order of 20% has been shown to result in practical design values (see Section 3.4). The coupling beams should then be preliminarily proportioned according to provisions in Section 5.

Step 5 – Check Drift Demands: Deflection limits may be selected in any rational manner or be based on appropriate specifications, e.g. FEMA-450 (2003). For example, based on current practice (ACI 2008 Section C21.9.6.2), a drift ratio limit of $\delta_H = 0.007$ is inferred for wall piers at the Life Safety performance level, which can be used for preliminary proportioning.

Once the appropriate deflection limit has been selected, construct an elastic model of the system as shown in Figure 13. Choose appropriate properties for the analysis

[1] "significant", in this case, may be defined by FEMA 356 as the case where the story shears found using only the fundamental mode are no less than 77% of those found using a linear dynamic procedure accounting for least 90% of the modal mass.

model of the HCW system as outlined in Section 2.2. Recommendations for effective member properties are given in Section 3.2. If the deflection limit is not satisfied, change the configuration by increasing the wall dimensions or changing the coupling beam distribution and iterate until the deflection limit is satisfied. Alternatively, the coupling ratio can be increased, requiring the designer to revisit Step 2.

Step 6 – Force Distribution in System: To compute the force distribution within the system, the capacity design method as proposed for eccentrically braced frames (Popov et al. 1989) is recommended. To obtain the force distribution in the model, it is recommended that the end restraints be released for all coupling beams, and the coupling beam end forces be applied to the wall piers as shown in Figure 13. The coupling beam shear force, V_i, and end moment, M_i, that must be applied at each level, i, are:

$$V_i = V_{beam,i} \tag{9}$$

$$M_i = \frac{gV_{beam,i}}{2} \tag{10}$$

Step 7 – Preliminary System Design: design the wall piers for the sum of the gravity loads, cantilever wall forces and coupling actions (Equations 5 and 6, above). Gravity loads associated with wall piers are based on tributary area. It is noted that most HCWs will have a surrounding gravity frame and thus the loads may be little more than the dead load of the wall piers themselves.

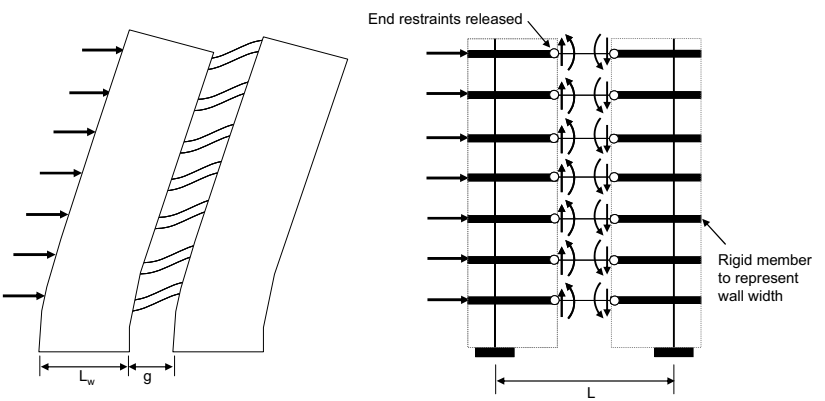

Figure 13: Proposed elastic model to be used for preliminary proportioning of HCW systems

4.5 Acceptance Criteria

FEMA-356 (2000) provides tables for acceptance criteria for common structural systems and their elements. The values provided in FEMA-356 are for existing structures and may underestimate the capacity of well-detailed new construction (Harries et al. 2004b and Xuan and Shahrooz 2005). These values are therefore considered conservative and are recommended for performance-based design of hybrid coupled wall systems until more appropriate acceptance criteria become available.

4.5.1 Coupling Beams

Coupling beam response is expected to be similar to shear link response in eccentrically braced frames (EBF). As such, the acceptance criteria for shear links in FEMA-356 Tables 5-5 and 5-6, based upon plastic rotation angles, are recommended for links that meet the design criteria in Section 5. In applying the EBF criteria to hybrid coupling beams, it is important that the effective length of the beam – as described by Equation 2 in Section 3.2 – is used. To be consistent with recommendations in this document, nominal coupling beam strengths should be substituted for expected strengths in the FEMA-356 equations.

4.5.2 Reinforced Concrete Wall Piers

Reinforced concrete wall response shall be considered to be dominated by flexural action as defined in FEMA-356 Section C6.8.1. As such, their performance should be judged based on acceptance criteria in FEMA-356 Tables 6-18 and 6-20. The permitted plastic hinge rotations (FEMA-356 Tables 6-18) and *m*-factors (FEMA-356 Tables 6-20) are a function of the axial load acting on the piers. To be consistent with recommendations in this document, the force P in these equations should be calculated as follows.

For the Compression Pier: Add the factored gravity load to the summation of the nominal shear capacities of the coupling beams multiplied by $1.1R_y$:

$$P = 1.2DL + 0.5LL + \left| \Sigma 1.1 R_y V_n \right| \quad [1] \tag{11}$$

To account for the detrimental effects of beam overstrength and to ensure the axial stability of the wall pier, the following criteria must be satisfied for the compression pier:

$$\frac{(A_s - A_s^{'}) f_y + P}{t_w l_w f_c^{'}} \leq 0.35 \tag{12}$$

For the Tension Pier: Compute the factored gravity load minus the summation of the nominal shear capacities of the coupling beams:

$$P = 0.9DL - \left| \Sigma 1.1 R_y V_n \right| \tag{13}$$

[1] $P = 1.2DL + 1.0LL + \Sigma 1.1 R_y V_n$ when $LL_0 > 100$ psf

4.5.3 Beam-Wall Connection

Connections designed according to the recommendations in Section 5 shall be expected to implicitly satisfy the acceptance criteria.

4.6 Design Process

The recommended design process using the PBDM is as follows:

1. Decide whether to use linear elastic or nonlinear analysis according to information in Section 4.2
2. Conduct a preliminary design based on the method outlined in Section 4.4. The preliminary design process may require iterations to satisfy preliminary drift and strength limits.
3. Construct a suitable model according to recommendations in Section 4.3.
4. Analyze the model using the appropriate analysis procedures outlined in FEMA-356 Section 3.3.
5. Check acceptance criteria according to Section 4.5 to ensure that the assumed design is satisfactory. If the acceptance criteria are not met, iterate until an acceptable design is achieved.
6. If a steel frame is used in conjunction with the wall, proportion the frame according to provisions in Section 3.1 and AISC-Seismic (2005).

5 Component Design

Design procedures for the various structural components of hybrid coupled walls are outlined in this section.

5.1 Coupling Beam Design

Coupling beams must be detailed to undergo substantial inelastic deformation reversals. Their strength and ductility should be carefully tuned along with the strength and ductility of the reinforced concrete wall piers to achieve good system economy and acceptable structural behavior.

Steel coupling beams are designated as protected zones as specified in AISC Seismic Section 7.4. Well established guidelines for shear links in eccentrically-braced frames (AISC Seismic 2005) are recommended for design (AISC Seismic Section 15.2) and detailing (AISC Seismic Section 15.3) of steel coupling beams.

The expected coupling beam rotation angle plays an important role in the required beam details such as the provision of stiffeners. This angle can be computed from application of the PrDM outlined in Section 3 or the PBDM outlined in Section 4. In either case, for an interstory drift angle of θ_d (equal to the computed story drift divided by the story height), the coupling beam rotations are:

$$\theta_b = \frac{L-g}{g}\theta_d \tag{14}$$

Where L is the distance between wall centroids, and g is the effective distance between the walls accounting for wall concrete cover spalling (Equation 2 in Section 3.2).

In addition to in-span stiffener requirements and detailing requirements prescribed by AISC Seismic (2005), face bearing plates must be provided at the face of the reinforced concrete wall. Face bearing plates take the form of full-width stiffeners located on both sides of the web – in effect, closing off the opening in the concrete form required to install the beam. Face bearing plates provide confinement and assist in transfer of loads to the concrete through direct bearing. These stiffeners are detailed based on AISC requirements (AISC Seismic 2005).

5.1.1 Composite versus Non-Composite Coupling Beams

Since the beams are protected zones in the AISC Seismic (2005) sense, they should not be made composite with the slab through the action of welded shear studs.

Previous research on steel-concrete composite coupling beams (Gong and Shahrooz 2001a,b,c) indicates that nominal encasement around steel beams provides beneficial effects, e.g., it improves resistance against flange and web buckling. However, the encasement is expected to deteriorate during strong seismic shaking, substantially altering the strength and stiffness of the coupling beams, which complicates the

system design process. For this reason, it is recommended that the steel coupling beams not be encased in concrete.

Nonetheless, if the beams are encased, the additional stiffness and strength due to encasement need to be taken into account in design. Stiffness based on gross transformed sections should be used to calculate the upper bound values of demands in the walls, most notably wall axial force. The cracked transformed section moment of inertia may be used when deflection limits or coupling beam shear angles are checked. As discussed in Section 5.2.1., the required embedment length needs to also account for the effects of encasement.

5.1.2 Coupling Beam Bracing

The bracing requirements for coupling beams are similar to those for shear links in eccentrically braced frames. Section 15.6 of the 2005 AISC Seismic Provisions specifies that lateral bracing shall be provided at both the top and bottom link flanges at the ends of the link. The reinforced concrete pier, acting in conjunction with the floor slab, can be counted upon to provide adequate lateral bracing at the top and bottom of the coupling beams at the faces of the walls.

5.2 Beam-Wall Connection Design

The coupling beam must be embedded in the walls such that its full capacity can be developed. Beam-to-wall connection detailing considerations should include requirements for attachments to the structural steel beam and detailing of transverse and longitudinal reinforcement in the connection region. Figure 14 shows a variety of beam-to-wall connections covered by these recommendations. For beams embedded in the plastic hinge regions of the wall piers, wall pier transverse reinforcement must be passed *through the web of the coupling beam* (an example is shown in Figure 4).

5.2.1 Embedment Length Calculation

Several models have been proposed for calculating connection moment capacity or for calculating minimum beam embedment length, L_e, to prevent a bearing failure. These are primarily based on models previously developed for connections between steel brackets and reinforced concrete columns (PCI Design Handbook 1999; Marcakis and Mitchell 1980; Mattock and Gaafar 1982).

It is recommended that the embedment length, L_e, required to develop the nominal coupling beam shear strength, V_n (as defined in AISC Seismic Section 15.2b), be calculated using the model proposed by Mattock and Gaafar (1982). When applying this method, the beam-wall connection must be designed to resist the coupling beam nominal strength magnified by $1.1R_y$ to account for the expected material strength and strain hardening, that is:

$$V_e = 1.1R_y V_n \tag{15a}$$

In case of composite coupling beams, the value of V_e is modified from the expression proposed by Gong and Shahrooz (2001a,b,c) as follows:

$$V_e = 1.1R_yV_n + 1.56V_{RC} = 1.1R_yV_n + 1.56\left(0.167\sqrt{f_c'}b_{wC}d_C + \frac{A_v f_{yr} d_C}{s}\right) \quad (15b)$$

The strength model is based on mobilizing an internal moment arm between bearing forces C_f and C_b as shown in Figure 15.

A parabolic distribution of bearing stresses is assumed for C_b, and C_f is estimated by a uniform stress equal to $0.85f'_c$. The bearing stresses are distributed over the beam flange width, b_f. Following these assumptions and calibrating against experimental data, the required embedment length, L_e, may be determined from:

$$V_e = 4.05\sqrt{f_c'}\left(\frac{t_w}{b_f}\right)^{0.66}\beta_1 b_f L_e\left[\frac{0.58-0.22\beta_1}{0.88+{}^{g}/_{2L_e}}\right] \quad (16)$$

Where β_1 is ratio of the average concrete compressive strength to the maximum stress, as defined in ACI 318-08. Note that f_c' in this equation is in MPa. The value of g may be taken as g_{clear} (i.e., the clear span) or as $g_{clear} + 0.6L_e$ (i.e., to be consistent with Equation 2). The resulting values of L_e from either approach will essentially remain unchanged.

5.2.2 Wall Boundary Regions at Beam Embedment

If the wall boundary element is reinforced with longitudinal and transverse reinforcing bars, the typical connection involves embedding the coupling beam into the wall and interfacing it with the boundary element, as shown in Figure 14.

In addition to boundary element reinforcing, embedded steel members should also be provided with vertical "transfer bars" welded to the beam flanges to assist in the transfer of vertical forces and thus improve the embedment capacity (PCI 1999; Shahrooz et al. 1992, 1993). The vertical bars may be attached to the flanges using mechanical half couplers which are welded to the flanges. Two sets of transfer bars are recommended: the first pair placed in a region to approximately coincide with the location of wall longitudinal bars closest to the wall face, and the second pair placed in a region near the end of the embedment length a distance no less than two times the diameter of the half coupler from the end of the embedment. The cross-sectional area of transfer bars required in each region of the embedded length is computed using Equation 17. However, the total cross-sectional area provided in both regions (at top and bottom flanges, need not exceed that given by Equation 18.

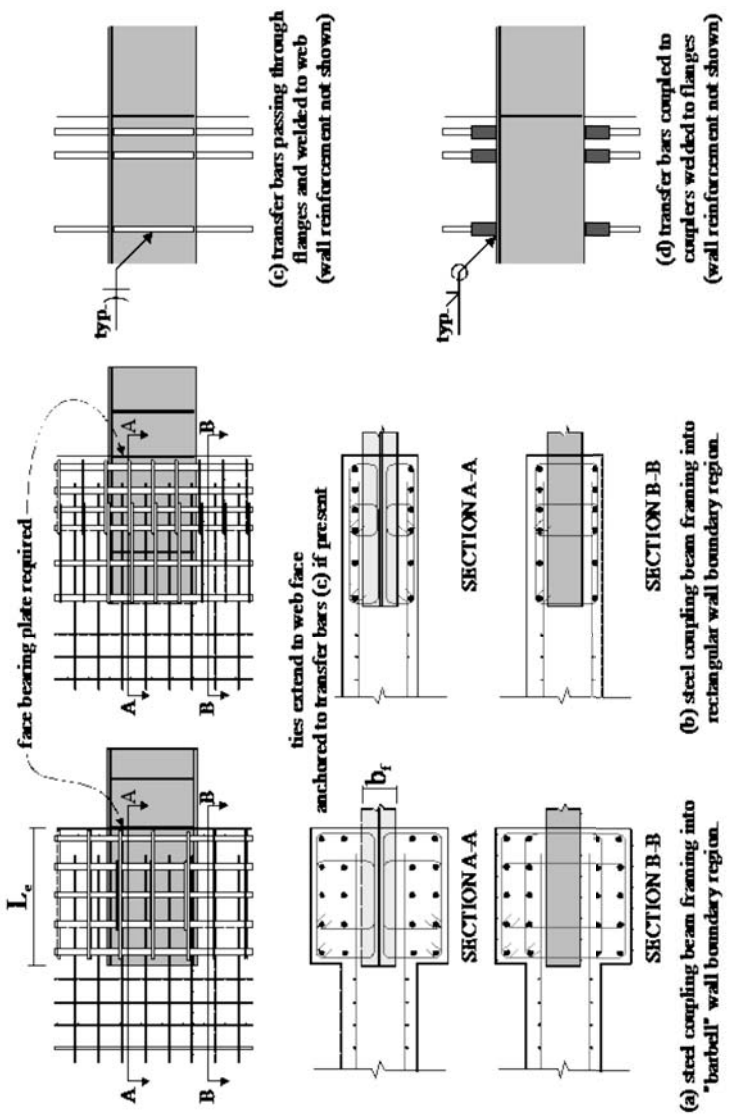

Figure 14: Connection details for HCW systems falling outside the plastic hinge regions of the walls. For those connections in the plastic hinge regions, transverse confinement reinforcement will pass through the coupling beam web.

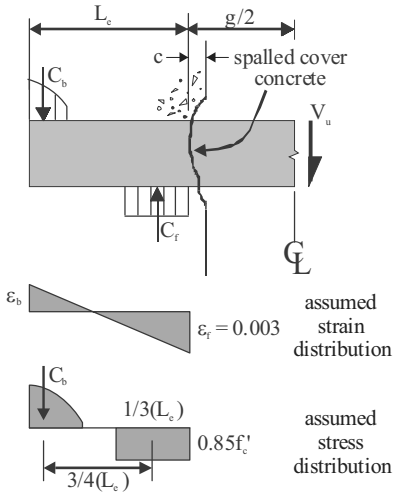

Figure 15: Method for determining embedment capacity.

$$A_{tb} \geq 0.03 f_e' L_e \left(\frac{b_f}{f_y}\right) \tag{17}$$

$$\sum A_{tb} < 0.08 L_e b_w - A_{sel} \tag{18}$$

If these transfer bars are provided with adequate tension development length, they may be engaged in resisting the embedment stresses shown in Figure 15. In such a case, the required embedment may be effectively reduced (Qin 1993). The use of such transfer bars significantly improves the energy dissipation characteristics of coupling beam-wall connections (Gong and Shahrooz 2001a,b). To ensure that the calculated embedment length is sufficiently large to avoid excessive inelastic damage in the connection region, it is recommended by Harries et al. (1997) and Shahrooz et al. (1993a,b) that the contribution of attached "transfer bars" be neglected when calculating the required embedment length (Equation 16).

Harries et al. (1997) recommend that two-thirds of the required vertical wall boundary element reinforcement be located within a distance of one half the embedment length from the face of the wall. Furthermore, the width of the boundary element steel should not exceed 2.5 times the coupling beam flange width. Satisfying these requirements will provide adequate control of the gaps that opens at the beam flanges upon cycling (Harries et al. 1992, 1997). With typical boundary element designs, these requirements are easily met.

Additionally, it is necessary to provide good confinement in the region of the embedded web. For relatively thin walls, confinement may be accomplished using

hairpins and cross ties parallel to the web, as shown in Figure 14. Additionally, vertical wall boundary element reinforcement in this region may also be relied upon to provide significant confinement to the embedded region (Harries et al. 1997).

For wider walls or those having "bar bells" at their toes, confinement of the concrete between embedded flanges requires additional reinforcing. Despite its use in a few installations (as discussed in Harries and Shahrooz 2005), it is not necessary, nor is it practical, to pass boundary element reinforcing through the web of the embedded coupling beam (as shown in Figure 4). A practical alternative to the practice of passing ties through the web is to utilize hooked ties on either side of the web and a short vertical bar between the flanges to anchor the ties (Lehmkuhl 2002).

Shear studs arranged along the embedded flanges and webs have also been used to assist in the transfer to horizontal loads and confinement of the local embedment region concrete. The efficiency of studs to transfer moment from the coupling beam into the wall in this manner has not been investigated. However, the use of studs on the embedded web represents a practical alternative to enhancing confinement in this area. Regardless of how confinement to the embedment region is provided, confinement requirements for the vertical wall reinforcing must also be met.

5.2.3 Top Beam-Wall Connections

At the top of the core wall piers, there is no reaction force available for the concrete compression block generated by the top flange of the embedded coupling beam (C_b in Figure 15). In many cases only a concrete slab is present above the top coupling beam and there will be insufficient capacity to develop the embedded beam in the manner shown in Figure 15. In this case, a strut-and-tie (ACI 2008, Appendix A) approach to detailing the topmost embedment region is appropriate. It is necessary to provide sufficient anchored vertical steel (usually U-ties) to develop the tie necessary to react the embedment forces. Figure 16 shows such an idealization of such a detail. In order to mitigate "blow out" of the top slab, the vertical U-ties should be anchored a distance of at least s/2 (where s is the resulting tie spacing) above the coupling beam flange to allow the compressive strut to be adequately developed (see enlargement in Figure 16). Additionally, the ties should be spaced no farther apart than the smaller of $t_w/2$ or 12 inches (where t_w is the thickness of the wall). The ties should extend along the entire development length and should engage the top slab reinforcement.

5.2.4 Joint Constructibility Issues

The wall vertical reinforcement must be placed such that the coupling beam can be embedded in the wall piers. This issue is particularly relevant if wall boundary elements are needed. Unless the wall piers are barbell shaped, the length of the boundary element may have to be extended so that the required amount of boundary element vertical reinforcement can be provided only with two curtains of reinforcement placed along the sides of the coupling beam flanges. The use of barbells allows more flexibility in how many curtains of wall boundary element vertical reinforcement can be placed without interfering with the embedded coupling beam (see Figure 14).

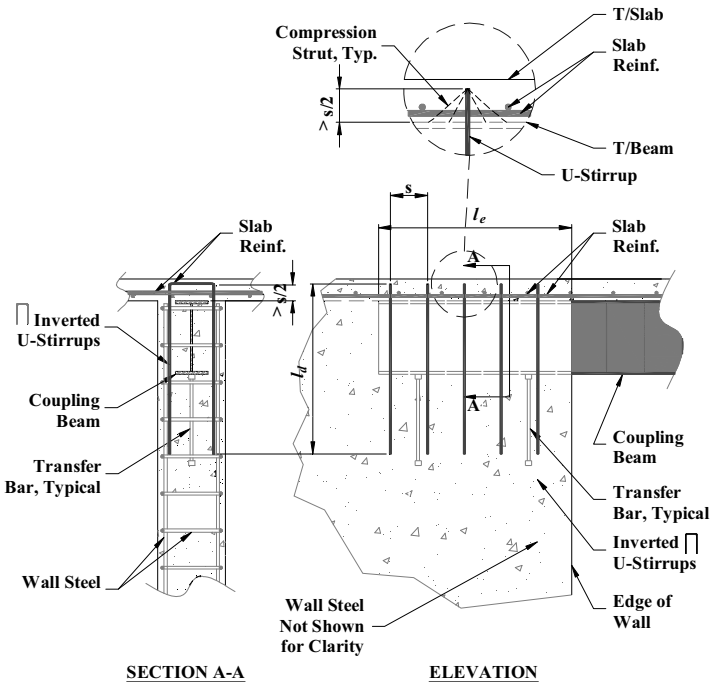

Figure 16: Top Wall-Beam Connection (no over-run)

5.3 Wall Pier Design

Reinforced concrete wall piers should be designed as shear walls according to the recommendations given in this section.

5.3.1 Flexural and Axial Strength Interaction

Similar to reinforced concrete columns subjected to combined axial load and moment, flexural strength of the wall piers should be computed based on ACI-318 Chapter 10. For flanged walls, tension flange reinforcement and, to a lesser extent, concrete contribution in the compression flanges significantly increases wall flexural capacity and should therefore be considered. Section 2.2.1 recommends the effective flange width for flanged sections. In lieu of those recommendations, the provisions in ACI Section 21.9.5.2 could be used.

5.3.2 Base Shear Magnification

For flexural walls in the nonlinear range of response during an earthquake, the maximum base shear demand can be significantly greater than that estimated using a fundamental mode inertial force distribution (e.g., Ghosh and Markevicius 1990; Eberhard and Sozen 1993; Otani et al. 1994; Hassan and El-Tawil 2004). This results as higher modes of vibration may cause the resultant inertial force to be located closer

to the wall base than the fundamental mode inertial force resultant, increasing the shear-to-overturning moment ratio at the base of the structure.

The base shear magnification factor for coupled wall structures can be estimated using a method developed for uncoupled wall systems by Kabeyasawa (1993) and Aoyama (1993). In this method, the maximum base shear demand, $Q_{w,max}$ is estimated as the sum of a fundamental mode component $Q_{1,max}$ and a higher mode component $Q_{h,max}$ as (Shen et al. 2006):

$$Q_{w,\max} = Q_{1,\max} + Q_{h,\max} \tag{19}$$

The fundamental mode and higher mode components are estimated as:

$$Q_{1,\max} = M_{wu} / H_1 \tag{20}$$

$$Q_{h,\max} = D_m m_w (PGA) \tag{21}$$

where:

$$D_m = 1 - m_{eff} / m_w + 0.7 m_{eff,2} / m_w \tag{22}$$

where, M_{wu} is the maximum base moment strength of the coupled wall structure, H_1 is the resultant height of the fundamental mode inertial force distribution (or a fundamental-mode-based equivalent lateral force distribution), PGA is the peak acceleration of the ground motion, and m_w, m_{eff}, and $m_{eff,2}$ are the total mass, effective fundamental mode mass, and effective second mode mass assigned to the coupled wall structure, respectively.

Current US practice does not recognize the effects of base shear magnification. However, a more conservative estimate of the design base shear can be obtained by increasing the computed design base shear by the magnification factor, $Q_{w,\max} / Q_{1,\max}$.

5.3.3 Wall Shear Strength

Wall nominal shear strength should be computed based on ACI-318 Section 21.9.4.1. The minimum horizontal and vertical reinforcement shall satisfy the requirements of ACI-318 Sections 21.9.2 and 21.9.4.3. The maximum nominal shear strength that a wall or a series of wall piers can develop shall not exceed the limitations of ACI-318 Sections 21.9.4.4 and 21.9.4.5.

5.3.4 Special Detailing of Shear Wall Boundary Elements

Wall pier demands in coupled core wall systems have distinct characteristics relative to those assumed in the seismic detailing provisions given in Chapter 21 of ACI 318 (2008); specifically, ACI 318 provisions 21.9.6.2 and 21.9.6.3 which prescribe methods for determining the need for “special” boundary elements. Neither method

for determining the need for special boundary elements (ACI 318 Sections 21.9.6.2 and 21.9.6.3) is recommended for wall piers in coupled core wall systems.

ACI 318 Section 21.9.6.2 follows from a displacement-based design approach for a cantilevered wall where the design displacement at the top of the wall is directly associated with the rotation at the base of the wall where a single flexure-critical section is assumed. Due to coupling action, it may not be reasonable to assume that the only critical section for flexure is at the base of the wall pier as it is for conventional cantilever piers. The implication of this observation is that for coupled walls it is not necessarily valid to relate the lateral deflection of the system to the wall rotation. The second method for determining the need for special boundary elements considers the extreme fiber concrete compressive stresses computed assuming a linear distribution of stress over the depth of the wall gross cross-section. The nature of coupled wall behavior and the expected moment distribution from tension to compression wall render such a simplified approach inappropriate for such structures.

Nonetheless, special boundary elements are required in wall piers when the flexural demands on the wall piers induce extreme fiber concrete compressive strains large enough to cause crushing of concrete in the compression zone. Concrete spalling in the boundary zone of a wall pier diminishes the stability of boundary element vertical reinforcement. Therefore, closely-spaced ties around the vertical bars are required to prevent vertical bar buckling, and to provide sufficient load-carrying capacity, toughness, and ductility. For HCWs, it is recommended that special boundary elements be provided when extreme fiber concrete compressive strains, at design displacements, exceed 0.003. The extreme fiber concrete compressive strains should be determined using cross-sectional fiber analyses incorporating rational constitutive material properties as described in Section 2.2.1. Critical strain checks should be made at each floor level, and locations over the height of the structure where inflection points in the wall curvature are anticipated. When using PrDM as described in Chapter 3, it should be noted that the wall overstrength factor varies over the height of the structure, and varies differently depending on the distribution of coupling beam shear capacity. Therefore, when determining the design loads for the wall piers at a particular floor level using PrDM, wall overstrength computed for the floor level being considered should be used. Depending on the coupling beam capacity distribution over the height of the structure, extreme fiber concrete compressive strains in the wall piers over the height of the structure may not be intuitively assumed to decrease in upper floor wall piers. For example, when lower capacity coupling beams are used in the upper floors, inter-story drift may be appreciable leading to relatively large curvature demands in the upper level wall piers.

Minimum wall boundary detailing requirements of ACI 318 section 21.9.6.5 still need to be met if special boundary elements are determined not to be needed.

5.3.5 Force Transfer at Base of Wall

All design axial, flexural, and shear forces computed at the base of the wall piers should be sufficiently transferred to the supporting foundation in accordance with the

provisions provided in ACI-318 Section 15.8. When net axial tensile forces are present in the wall piers, which is common in HCW systems, wall pier vertical reinforcement in addition to that provided for lateral force resistance, as required by ACI-318 Section 11.6.7, should be provided to resist the wall pier axial tensile forces. Furthermore, foundation systems should be sized and proportioned to sufficiently transfer the design forces and overturning moments to the supporting soil such that compressive soil bearing pressures are present beneath the entire foundation base, and the allowable soil bearing pressures are not exceeded.

6 Alternative Hybrid Wall Systems

6.1 Unbonded Post-Tensioned Coupled Wall Systems

Recent research has investigated the use of post-tensioned steel beams to couple reinforced concrete walls (Shen and Kurama 2002; Kurama and Shen 2004; Kurama et al. 2006; Shen et al. 2006a,b). As an example, Figure 17a shows a multi-story coupled wall system and Figure 17b shows a floor-level subassemblage that includes a steel coupling beam and the adjacent wall regions. The coupling of the structure is achieved by post-tensioning the beams and the wall piers together, without embedding the beams into the walls. The post-tensioning (PT) force is provided by high-strength multi-strand tendons that are placed inside the wall piers and inside (in the case of hollow beam cross sections, such as a box-section) or outside (in the case of open beam cross sections, such as an I-section) the coupling beams. The PT steel is deliberately not bonded to the concrete by placing the tendons inside ungrouted ducts or by using strands that are wrapped inside grease-impregnated plastic sheathing. This type of construction, where the PT steel is anchored to the structure only at the ends, is called "unbonded" post-tensioning and has two important advantages: i) it results in a close-to-uniform strain distribution in the tendon, thus, significantly delaying or preventing the nonlinear behavior of the steel and maintaining the initial prestress under cyclic loading; and ii) it significantly reduces the tensile stresses transferred to the concrete, thus reducing cracking.

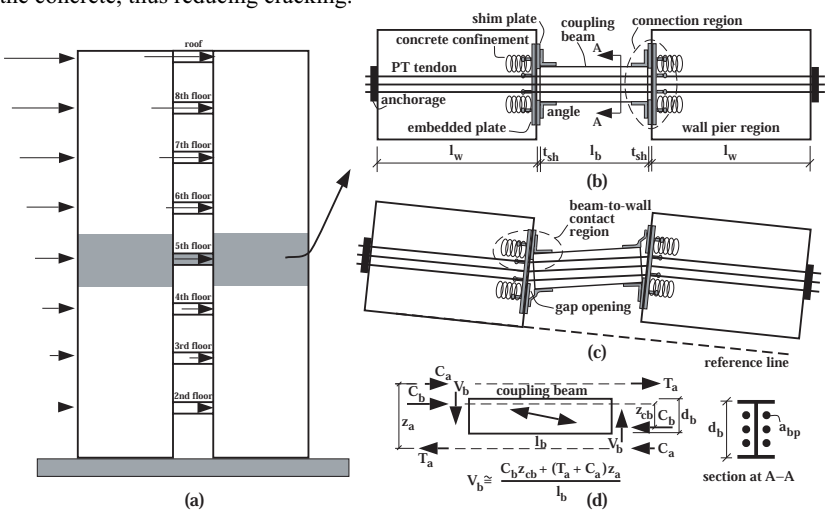

Figure 17: Post-tensioned hybrid coupled wall structures – (a) multi-story wall system; (b) floor subassemblage; (c) idealized exaggerated displaced shape; and (d) coupling forces.

Figure 17c shows an idealized exaggerated displaced shape of the subassemblage under lateral forces acting on the wall piers from left to right. During lateral

displacements into the nonlinear range, the behavior of the structure is governed by the opening of gaps at the beam-to-wall interfaces. The gap opening behavior results in a geometric reduction in the lateral stiffness of the system (i.e., geometric nonlinearity as compared with material nonlinearities) and allows it to soften and undergo large nonlinear rotations without significant damage. As depicted in Figure 17d, the coupling forces develop from the formation of a large diagonal compression strut in the beam. The coupling shear force, V_b can be controlled by the PT force P_b (which controls the diagonal compression strut, C_b), the beam depth d_b, and length l_b.

The beam-to-wall connection regions in an unbonded post-tensioned coupling system include steel plates and concrete confinement reinforcement (e.g., spirals or rectangular hoops) to distribute the compressive stresses due to the PT force. In addition, various methods utilizing the gap opening displacements can be used to provide energy dissipation to the structure. For example, the system in Figure 17 includes steel top and seat angles at the beam ends, where the desired behavior is yielding of the angles with little yielding and damage in the beam and wall piers. In addition to energy dissipation, the angles also provide a part of the coupling resistance (C_a and T_a in Figure 17d), prevent sliding of the beam at the ends (together with friction resistance against sliding; as induced by post-tensioning), and serve as temporary beam supports during construction. The yielded angles can be replaced after a large earthquake.

Eleven floor-level unbonded post-tensioned hybrid coupled wall subassemblages were tested using the setup in Figure 18a (Kurama et al. 2006; Shen et al. 2006b). Each specimen included a coupling beam and the adjacent wall pier regions at 50% scale. The left wall region, referred to as the reaction block, was fixed to a strong floor. Two actuators were used to displace the right wall region (referred to as the load block) vertically such that the rotation of the block was prevented as the beam was rotated through a quasi-static reversed-cyclic history. These conditions result in displacements similar to the displacements with respect to the "reference line" in Figure 17c.

The cyclic beam chord rotation history targeted during one of the tests (Test 3, see Kurama et al. 2006; Shen et al. 2006b) is depicted in Figure 18b, where the chord rotation is defined as the relative vertical displacement between the coupling beam ends divided by the beam length. Figure 18c shows the coupling beam shear force versus chord rotation (V_b-θ_b) behavior from the test specimen. Only the first cycle during each set of displacement cycles of equal amplitude is shown, except where significant differences occur in the subsequent cycles. The hysteresis loops demonstrate desirable seismic characteristics with stable behavior up to θ_b=8% and significant energy dissipation. The straight dashed line in Figure 18c shows the theoretical initial (i.e., linear-elastic) stiffness of the subassemblage assuming fixed beam-to-wall connections (representing an embedded steel beam). It is observed that, as a result of post-tensioning, the initial lateral stiffness of the test beam before the initiation of gap opening is similar to the initial stiffness of an embedded steel coupling beam.

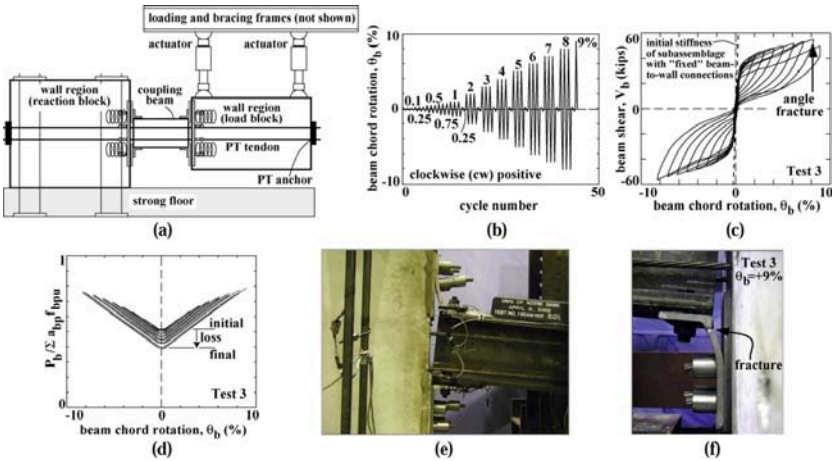

Figure 18: Subassemblage experiments – (a) test set-up; (b) beam chord rotation history; (c) beam shear force versus chord rotation behavior; (d) total beam PT force; (e) beam end view; and (f) angle fracture.

The hysteresis loops in Figure 18c indicate that the beam PT strands provide a restoring force that closes the gaps and pulls the beam back towards its undisplaced position upon unloading, resulting in a large self-centering capability with almost no residual displacement. The initial stiffness of the subassemblage is preserved even after unloading from very large nonlinear rotations. The sum of the coupling beam PT forces, P_b measured during the test (normalized with the total design maximum strength of the PT strands, $P_{bu}=\Sigma a_{bp} f_{bpu}$) is plotted in Figure 18d. Before the initiation of gap opening, the total force in the PT strands is similar to the initial force. As the specimen is displaced, the strand forces increase, thus resisting gap opening. Prestress losses are observed upon unloading from increased displacements; however, these losses are small because of the use of unbonded PT strands. Note that the structure displacements in Figure 17c are exaggerated, resulting in a "kinked" appearance of the PT steel at the beam-to-wall interfaces. Under a "Design-Basis" Earthquake, the angle change in the tendons at the beam-to-wall interfaces is expected to be small. It would be possible to keep the PT tendons straight between anchors by placing the tendons inside oversized ungrouted ducts; however, this is not considered to be necessary since no undesirable behavior along the length of unbonded PT strands has been observed during previous experiments (Priestley and MacRae 1996; Kurama et al. 2006; Shen et al. 2006b; Morgen and Kurama 2004, 2007). The most critical location for unbonded PT tendons is inside the anchors, where premature strand slip behavior and strand wire fractures have been observed during some of the experiments described in Kurama et al. (2004, 2006) and Morgen and Kurama (2007). A short length of the PT tendons can be bonded to the surrounding concrete at each end to eliminate any premature strand failures inside the anchors.

Figure 18e shows a photograph of the test specimen near the reaction block at a beam chord rotation of θ_b=+8%. It can be seen that the opening of gaps at the beam ends results in the yielding of the top and seat angles in tension and compression, thus, providing energy dissipation under reversed-cyclic loading. During the experiment, initiation of low cycle fatigue cracks was observed in the vertical legs of the tension angles at about θ_b=7%. The cracks occurred at the critical section adjacent to the fillet. The specimen was able to sustain three cycles at θ_b=8% with a steady, but not excessively large, reduction in strength and post-softening stiffness (see Figure 18c). This reduction in stiffness and strength occurred due to increased cracking and necking of the vertical legs of the tension angles.

The ultimate failure of the specimen eventually occurred as a result of the complete fracture of the vertical leg of the seat angle at the right (north) end of the beam when θ_b=+9% was reached for the first time. The resistance of the specimen at this stage was, approximately, 90% of the peak resistance. Figure 18f shows the fractured angle at θ_b=+9%. All four angles had sustained significant yielding at this stage, resulting in a considerable amount of energy dissipation in the structure. The damage in the beam and wall regions was negligible, with negligible compression yielding of the beam flanges and no cracking and/or spalling of the wall concrete. As shown in Figure 18e, the angle-to-wall connections performed well, allowing the angles to go through large nonlinear deformations without damaging the concrete. The angle-to-beam connections also behaved satisfactorily, with no slip between the angles and the beam up to θ_b=5% and negligible slip afterwards, indicating that the slip-critical angle-to-beam connection bolts were adequate. It may also be possible to weld the horizontal legs of the angles to the beam flanges to prevent any slip at the angle-to-beam connections. Slip between the coupling beam and the reaction and load blocks did not occur, demonstrating that the angles provided adequate vertical support to the beam together with friction resistance due to post-tensioning.

The experimental results summarized above were used to develop analytical models for floor-level unbonded post-tensioned hybrid coupled wall subassemblages (Shen and Kurama 2002; Shen et al. 2006a,b) and multi-story coupled wall structures (Kurama and Shen 2004). These models were then used to conduct a comprehensive analytical study on the seismic behavior and design of unbonded post-tensioned hybrid coupled wall structures (Shen et al. 2006a,b). In addition to the beam PT tendons, the use of PT steel running vertically over the height of the wall piers was also investigated (Kurama and Shen 2004).

The experimental and analytical research results developed by this project have shown that unbonded post-tensioned steel beams can be designed to provide significant and stable levels of coupling between concrete walls over large nonlinear reversed-cyclic lateral displacements. The test results demonstrate that the system has excellent stiffness, strength, ductility, and energy dissipation characteristics, with most of the damage occurring in replaceable beam-to-wall connection angles (or other yielding energy dissipation components placed at the beam ends). The beams

and the coupling regions of the wall piers do not receive any significant damage, and thus, do not require any significant repair after a large earthquake. Since the beams are not embedded into the wall piers, the construction of the coupling regions of the wall piers is relatively simple and the selection of the beam cross section size and shape is not restricted by the wall reinforcement. Note that, as a result of gap opening at the beam-to-wall interfaces, the coupling moment strength of an unbonded post-tensioned steel coupling beam is smaller than the moment strength of an embedded steel coupling beam with the same cross section. The increased building project costs associated with this strength reduction may be compensated by some of the construction advantages and reduced post-earthquake repair costs of unbonded post-tensioned systems. Furthermore, as an important benefit, the PT force results in a self-centered response with significantly reduced residual (i.e., permanent) displacements of the entire structure after a large earthquake. Based on these findings and considerations, it is concluded that unbonded post-tensioned steel beams provide an effective and feasible means to couple reinforced concrete walls in seismic regions.

6.2 Steel Coupling Beam with Fuse

In an effort to protect the wall piers from local damage around the coupling beams, a system involving a central fuse has been examined (Fortney et al. 2007a; Fortney 2005). The fuse is to act as a repairable or replaceable "weak link" where the inelastic deformations are concentrated while the remaining components of the system are to remain elastic. A schematic drawing of such a system is shown in Figure 19.

The larger shear capacity of the main section of the beam will have relative to the fuse is arbitrarily chosen. Previous tests (Fortney et al. 2006a; Fortney 2005) have examined fuses with 50% and 70% of the shear capacity of the main section. The flexural capacity of the main section is maintained for the fuse section. The fuse is interfaced with the main section through slip-critical bolted connections at the top and bottom flanges as well as at the web. The use of slip-critical connections is intended to prevent damage to the main section which would, in effect, compromise the intended behavior of the system. The length of the fuse, which is affected by the length of the splice plates, is minimized to reduce the demands in the flange and web splice plates and bolts. The moment of inertia of the splice plates must be greater than or equal to that of the main beam to avoid excessive stresses in the splice plates. The main section of the coupling beam, including its connection to the wall piers, is designed and detailed according to the aforementioned design methodology for steel coupling beams.

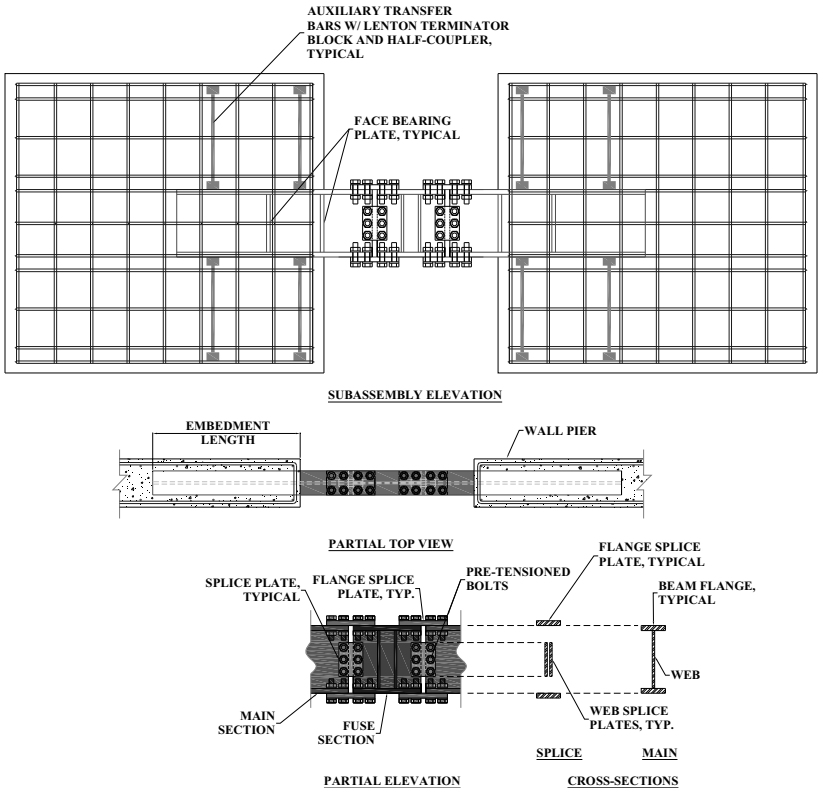

Figure 19: Schematic drawing of steel coupling beam with a central fuse

Limited tests (Fortney et al. 2007a,b; Fortney 2005) suggest satisfactory performance. Figure 20 shows the measured performance of the fuse steel coupling beam as shown in Figure 19. These tests highlighted the importance of weld quality particularly between the web and flanges at the ends of the beam sections.

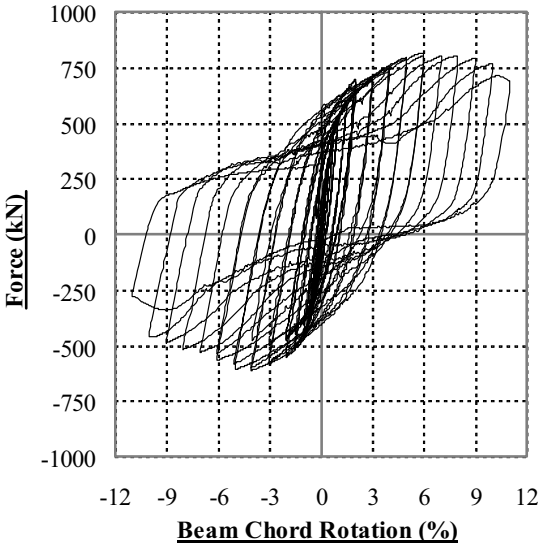

Figure 20: Shear force versus beam chord rotation for fuse steel coupling beam

6.3 Composite Shear Plate Coupling Beam

This alternative consists of a vertically-oriented steel plate encased in a conventionally confined concrete beam that relies on composite behavior to transfer coupling beam shear forces. Longitudinal reinforcement is provided to ensure flexural strength. The design methodology proposed by Fortney (2005) extended a model developed by Subedi (1989) by providing transverse reinforcement intended to contribute to the shear strength of the beam, as well as provide sufficient confinement of the concrete encasing the steel plate. Additionally, a variable is incorporated which gives the designer the ability to control the desired level of flexural strength versus shear strength to ensure shear dominant behavior of the section.

Shear plate coupling beam may be modeled as a deep composite girder with longitudinal reinforcement and vertical web plate. The recommended design methodology incorporates Tresca's maximum shearing stress theory to account for the shear/flexure interaction, and combines the shear resistance of the plate and transverse reinforcement. In practical design, the steel plate would be designed to resist the design shear forces. A detailed derivation of the recommended design equation is provided in Fortney 2005.

Plate stability is assumed to be provided by the surrounding confined concrete. Shear transfer between concrete and web plate is accomplished through the use of headed studs welded on both faces of the web plate. The size and spacing of the studs are computed based on standard procedures (AISC 2006; PCI Design Handbook, Edition 6), and are used in the clear span of the beam and connection regions. Considering the expected moment and shear diagrams for coupling beams, the minimum embedment

length of the web plate will be one half of the clear span. To ensure shear dominant behavior, and to minimize the required cross-sectional area of longitudinal steel, high strength longitudinal reinforcing bars will most likely have to be provided to resist the coupling beam design moment. A typical cross section is shown in Figure 21.

Limited tests (Fortney et al. 2006a and 2006b, Fortney 2005) indicate satisfactory performance so long as special care is made to ensure the quality of stud welds connecting the studs to the plate. Figure 21 shows the measured performance of the shear plate coupling beam.

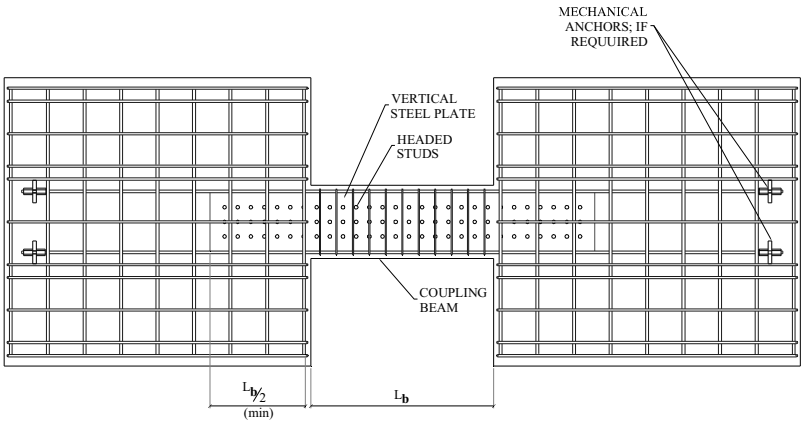

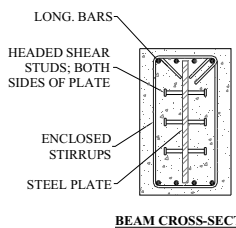

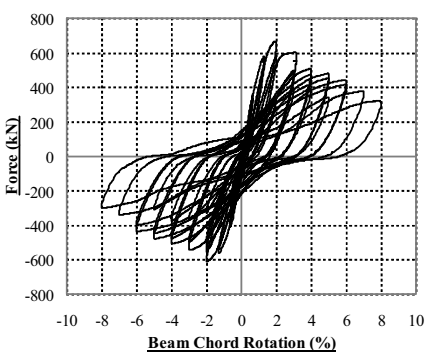

Figure 21: Schematic and measured performance of shear plate coupling beam

Appendix I: Development of Fundamental Wall Geometry

The following procedure is based on the continuous medium method and assumes elastic material properties. Details of this method are provided in Stafford-Smith and Coull (1991) and some additional derivations are presented in Harries et al. (2004). This Appendix describes a system having two coupled wall piers. Methods for simplifying multiple pier systems into equivalent two-pier systems are provided in Stafford-Smith and Coull (1991).

I.1 Geometric Description of HCW Behavior

Four fundamental parameters may be used to describe *elastic* coupled wall behavior: The first and second parameters are respectively, H, which represents the overall height of the building, and $CR_{elastic}$, which is the coupling ratio for the *elastic* system. The third and fourth parameters for a two wall system are given below:

$$\alpha = \sqrt{\frac{12 I_c L^2}{L_b^3 h I}} \tag{I.1}$$

$$k = \sqrt{1 + \frac{AI}{A_1 A_2 L^2}} \tag{I.2}$$

Where

I = sum of the moments of inertia of the individual wall piers ($I = I_1 + I_2$);
A = sum of the areas of the individual wall piers ($A = A_1 + A_2$);
L = distance between wall centroids;
L_b = length of coupling beam;
h = story height; and,
I_c is the effective moment of inertia of the coupling beam accounting for shear deformations:

$$I_c = \frac{I_b}{1 + \left(\frac{12 E I_b}{L_b^2 G A_b} \lambda \right)} \tag{I.3}$$

Where

I_b and A_b = gross moment of inertia and area of the coupling beam, respectively;
E and G = Young's modulus and the shear modulus of the coupling beam; and,
λ = shape factor, defined as the ratio of the plastic to elastic section moduli, Z_x/S_x.

In Equations I.1 through I.3, cracked section properties such as those proposed in Section 3.2.1 should be used.

The parameter α is a measure of the relative flexibility of the coupling beams and the walls. A low value of α indicates a relatively flexible coupling beam system. In such a case, the overall behavior of the system will be governed by the flexural response of the individual wall piers. A higher value of α leads to greater coupling (frame) action between the walls. The parameter k is a measure of the relative flexural to axial stiffness of the wall piers. This parameter has a lower limit of $k = 1$ representing axially rigid wall piers and varies up to values of about $k = 1.2$. It should be noted that a structurally and architecturally practical coupled structure will typically have a k value less than 1.1.

$$k\alpha H = \sqrt{\left(1 + \frac{AI}{A_1 A_2 L^2}\right) \frac{12 I_c L^2}{L_b^3 h I} H^2} \tag{I.4}$$

The parameter $k\alpha H$ in Equation I.4 may be interpreted as a measure of the stiffness of the coupling beams and is most sensitive to changes in either the stiffness or length of the coupling beam – that is, the α term. Furthermore, the $k\alpha H$ parameter may be used to determine the elastic coupling ratio, $CR_{elastic}$ (Chaallal and Nollet 1997) as:

$$CR_{elastic} = \frac{3}{k^2 (k\alpha H)^2} \left[\frac{(k\alpha H)^2}{3} - \cosh(k\alpha H) + \frac{\sinh(k\alpha H) - k\alpha H/2 + 1/k\alpha H}{\cosh(k\alpha H)} \sinh(k\alpha H) \right] \tag{I.5}$$

Typically, if $k\alpha H$ is less than 1, the structure is considered to have negligible coupling action ($CR_{elastic}$ < 20%) and behaves as an arrangement of linked walls resisting overturning almost entirely through flexure of the wall piers. For values of $k\alpha H$ greater than about 8 ($CR_{elastic}$ > 75%), the coupling beams are considered to be stiff and the structural response is dominated by that of the wall piers as described by the factor k. In this case, a flexible wall pier system (higher values of k) results in greater coupling action as the flexibility of the walls engages the frame action of the coupling beams. Incremental changes in the coupled response of the structure become negligible for values of $k\alpha H$ greater than about 8 ($CR_{elastic}$ > 75%). Global structural deformations, represented by the roof deflection, shown in Figure I-1 normalized by the roof deflection for a pair of linked cantilever walls, are also relatively unaffected beyond this value. If the coupling beams are rigid ($k\alpha H = \infty$) the structure behaves as a single cantilever wall.

I.2 Elastic HCW Behavior

The roof deflection, y_H, of a coupled wall having an inverse triangularly distributed lateral force varying from zero at the wall base to p at the roof is (Stafford-Smith and Coull 1991):

$$y_H = \frac{11 p H^4}{120 EI} \varsigma[k\alpha H] \tag{I.6}$$

The factor ς is the reduction in roof deflection affected by the coupling action compared to the roof deflection of a pair of linked walls subject to an inverse triangular lateral load having a magnitude at the roof of p: $y_H = \frac{11pH^4}{120EI}$; and is given as:

$$\varsigma = 1 - \frac{1}{k^2} + \frac{120}{11}\frac{1}{k^2(k\alpha H)^2}\left[\frac{1}{3} - \frac{1 + \left(k\alpha H/2 - 1/k\alpha H\right)\sinh(k\alpha H)}{(k\alpha H)^2\cosh(k\alpha H)}\right] \tag{I.7}$$

Thus to develop the curves used for preliminary wall geometry selection, Equations I.5 and I.7 are plotted against each other incrementing values of $k\alpha H$ (Figure I.1 and Figure 7). A value of k must be assumed. Practical values of k range from 1.05 to 1.1 and will not greatly affect the selection of preliminary wall geometry as shown Figure I.1.

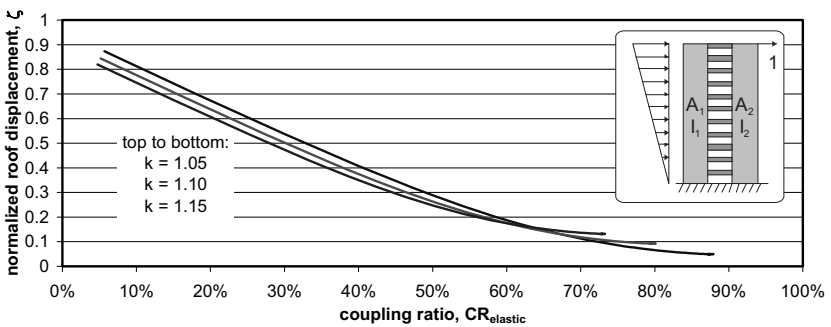

Figure I.1: Normalized roof deflections for inverse triangular load.

I.3 Elastic distribution of coupling beam shear demand

The distribution of shear in the coupling beams is represented by the shear flow in the theoretical coupling continuum (Stafford-Smith and Coull, 1991):

$$q = \frac{pH}{k^2 L}\xi\left[z/H, k\alpha H\right] \tag{I.8}$$

Recognizing that the integration of the coupling beam shear flow, q, is equal to the sum of the beam shears, ΣV_{beam}, the shear flow may be normalized by the beam shears induced by coupling given by Equation 6:

$$\sum_{i=1}^{N} V_{beam,i} = \frac{CR_{elastic}.OTM}{L} \tag{I.9}$$

Where the *OTM* for an inverse triangular load is given as:

$$OTM = pH^2/3 \tag{I.10}$$

Thus the normalized beam shear may be written as:

$$\frac{V_{beam}}{\sum V_{beam}} = \frac{3h}{CR_{elastic}k^2LH}\xi[z/H, k\alpha H] \tag{I.11}$$

This relationship, plotted for a number of building heights (H) and values of $CR_{elastic}$ is shown in Figure I.2. The so called, "pregnant" distribution of beam shear is clearly evident and is more pronounced as $CR_{elastic}$ increases.

Finally, ξ is defined as (Stafford-Smith and Coull 1991):

$$\xi = \left[\frac{\sinh(k\alpha H) - k\alpha H/2 + 1/k\alpha H}{(k\alpha H)\cosh(k\alpha H)}\cosh(k\alpha(H-z)) - \frac{\sinh(k\alpha(H-z))}{(k\alpha H)} + \left(1-\frac{z}{H}\right) - \frac{1}{2}\left(1-\frac{z}{H}\right)^2 + \frac{1}{(k\alpha H)^2}\right] \tag{I.12}$$

Where z varies from 0 at the base of the structure to H.

I.4 Preliminary Proportioning

The following method is intended to assist the designer in selecting fundamental CCW geometric parameters that will result in practical CCW behavior with fewer significant design iterations.

Step 1 – Define the coupling ratio for elastic conditions: $CR_{elastic} = \gamma CR$, where, *CR* is the coupling ratio as defined in Section 2 and γ is taken as:

$$\gamma = 1.75 \tag{I.13}$$

Step 2 – Select a target roof drift ratio, δ_H. Deflection limits may be selected in any rational manner or appropriate specifications could be specified. For example, based on current practice (ACI 2008), a drift ratio limit of $\delta_H = 0.007$ is recommended for wall piers at the Life Safety performance level, which can be used for preliminary proportioning.

Step 3 – Using the continuous medium method described in this Appendix and the assumption of elastic properties, design curves similar to those shown in Figure I.1 or Figure 7 may be developed. These figures are based on a pair of cantilever walls subject to an inverse triangular lateral load (different curves may be generated for any distribution including those based on modal combination). Since first mode response is assumed to dominate HCW behavior for the purposes of initial proportioning, design curves may be developed assuming an equivalent inverted triangular load distribution having a magnitude *p* at the roof. Additionally, in Figure 7, the curve

shown is based on the measure of relative wall pier properties corresponding to k = 1.1. For practical walls, k varies between about 1.05 and 1.1. Different values of k will result in the curve shifting upwards ($k < 1.1$) or downward ($k > 1.1$) as shown in Figure I.1.

Enter the design curve at the value of $CR_{elastic}$ and determine the ratio of the HCW roof drift to the drift of a linked cantilever system. This value, the "normalized roof deflection" in Figures I.1 or 7, is designated, ς, in the following equations.

Step 4 – Determine the preliminary wall geometry by the following procedure. The uncoupled (linked) cantilever elastic roof deflection associated with inverse triangular loading is:

$$y_H = \frac{11pH^4}{120E(I_1 + I_2)} \tag{I.14}$$

The, initially appropriate flexural stiffness values for the wall piers, I_1 and I_2 may be estimated by substitution into Equation I.15:

$$\frac{\delta_H H}{\varsigma} = \frac{11pH^4}{120E(I_1 + I_2)} \tag{I.15}$$

If two identical walls are coupled, the geometry of each wall is found to be:

$$I_{1required} = I_{2required} = \frac{\varsigma 11pH^3}{2\delta_H 120E} \tag{I.16}$$

Finally, the relationship between A and I is prescribed by Equation I.2 to satisfy the original assumption of k = 1.1. It has, however been shown that overall behavior is not particularly sensitive to the value of k so an initial assumption of k =1.1 is reasonable and enforcing the *A-I* relationship implied by Equation I.2 is unnecessary, particular in the initial design process.

Step 5 – having established a preliminary wall geometry, the expected coupling beam behavior may be assessed as discussed in Section I.3.

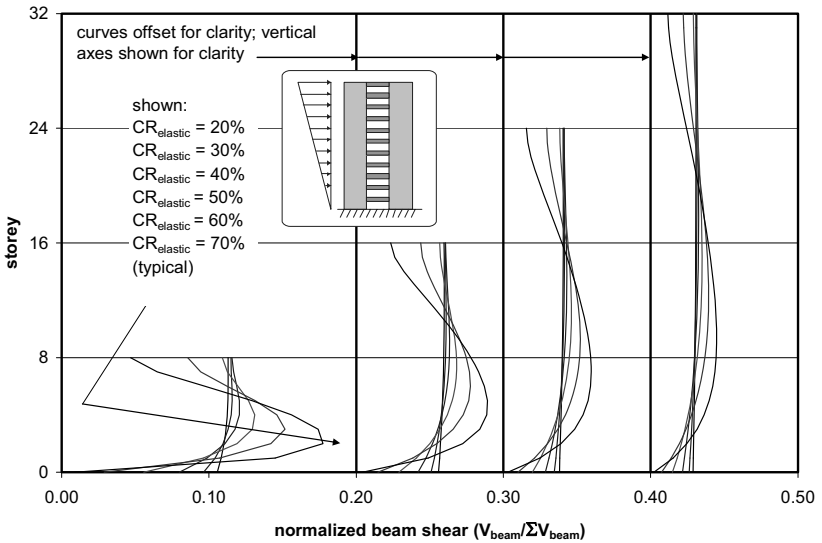

Figure I.2: Proposed distribution of normalized beam shear demands in coupled wall systems of different heights and with different $CR_{elastic}$.

Appendix II: References

Aktan, A. E. and Bertero, V. V. (1984), "Conceptual Seismic Design of Frame-Wall Structures." *Journal of Structural Engineering*, ASCE, 110(11), 2778 - 2797.

American Concrete Institute (ACI) Committee 318 (2008), "ACI 318-08 Building Code Requirements for Reinforced Concrete and Commentary." (ACI 318-08/ACI 318R-08), Farmington Hills, MI.

American Institute of Steel Construction (AISC) (2002), "Seismic Provisions for Structural Steel Buildings." Chicago, IL.

American Society of Civil Engineers (ASCE) (2005), SEI/ASCE 7-05 – "Minimum Design Loads for Buildings and Other Structures." American Society of Civil EngineersASCE, Reston VA.

Antonio, S., Rovithakis, A., and Pinho, R. (2002). "Development and verification of a fully adaptive pushover procedure." *Proc. of the 12th European Conference on Earthquake Engineering*, Paper No. 822.

Antonio, S., and Pinho, R. (2004). "Development and verification of a displacement-based adaptive pushover procedure." *Journal of Earthquake Engineering*, 8(5), 643-661.

Aoyama, H., (1993). "Earthquake Resistant Design of Reinforced Concrete Frame Buildings with 'Flexural' Walls," *Earthquake Resistance of Reinforced Concrete Structures*, A Volume Honoring Hiroyuki Aoyama, Editor: T. Okada, Department of Architecture, Faculty of Engineering, University of Tokyo, Japan, pp 78-100.

Bentz, E. C. (2000). RESPONSE 2000 Version 1.0.5. University of Toronto.

BSSC (1994), "NEHRP Recommended Provisions for the Development of Seismic Regulations for New Buildings, Part I: Provisions, Part II: Commentary, FEMA 222A and 222B." FEMA, Washington, DC.

BSSC (1997), "NEHRP Recommended Provisions for the Development of Seismic Regulations for New Buildings, Part I: Provisions, Part II: Commentary, FEMA 302 and 303" FEMA, Washington, DC.

Canadian Standards Association (CSA) (2004), "CSA A23.3-04 Design of Concrete Structures." Rexdale, Canada.

Chitty, L. (1947), "On the Cantilever Composed of a Number of Parallel Beams Interconnected by Cross Bars" *London, Edinburgh and Dublin Philosophical Magazine and Journal of Science*, Vol. 83, pp 685-699.

Chopra, A. K., and Goel, R. K. (2002). "A modal pushover analysis procedure for estimating seismic demands for buildings." *Earthquake Engineering and Structural Dynamics*, Vol. 31, pp 561-582.

Chopra, A. K., Goel, R. K., and Chintanapakdee, C. (2004). "Evaluation of a modified MPA procedure assuming higher modes as elastic to estimate seismic demands." *Earthquake Spectra*, 20(3), 757-778.

Deason J.D., Tunc G., and Shahrooz B.M. (2001). "Seismic Design of Connections Between Steel Outrigger Beams and Reinforced Concrete Walls." *Steel & Composite Structures – an International Journal*, 1(3), 329-340.

Eberhard, M. and Sozen, M., (1993). "Behavior-Based Method to Determine Design Shear in Earthquake-Resistant Walls." *Journal of Structural Engineering*, ASCE, 119(2), 619-640.

Elnashai, A. S. (2000). "Advanced inelastic (pushover) analysis for seismic design and assessment." *The G. Penelis Symposium*, Thessaloniki, Greece.

El-Tawil, S. and Deierlein, G. G. (2001). "Nonlinear analyses of mixed steel-concrete moment frames. Part I - beam-column element formulation. Part II - implementation and verification." *Journal of Structural Engineering*, ASCE, 127(6), 647-665.

El-Tawil, S., Kuenzli, C. M., and Hassan, M. (2002a). "Pushover of Hybrid Coupled Walls. Part I: Design and Modeling." *Journal of Structural Engineering*, ASCE, 128(10), 1272-1281.

El-Tawil, S. and Kuenzli, C. M. (2002b). "Pushover of Hybrid Coupled Walls. Part II: Analysis and Behavior." *Journal of Structural Engineering*, ASCE, 128(10), 1282-1289.

FEMA-450 (2003). "NEHRP Recommended Provisions for Seismic Regulations for New Buildings and Other Structures. Part 1 – Provisions.", *Building Seismic Safety Council*, Washington, D.C.

FEMA-356 (2000). "Prestandard and Commentary for the Seismic Rehabilitation of Buildings." FEMA 356/November 2000, *Building Seismic Safety Council*, Washington, D.C.

FEMA-350 (2000). "Recommended Seismic Design Criteria For New Steel Moment-Frame Buildings." FEMA 350/July 2000, *Building Seismic Safety Council*, Washington, D.C.

FEMA-273 (1997). "NEHRP Guidelines for the Seismic Rehabilitation of Buildings." FEMA 273/October 1997, *Applied Technology Council* (ATC-33 Project), Redwood City, California.

Fortney, P. J., Harries, K. A., and Shahrooz, B. M., (2008). "Design Compression Forces for Coupled Wall Structures." *Proceedings of the ASCE STRUCTURES 08 Congress*, Vancouver, April 2008.

Fortney, P. J., Shahrooz, B. M., Rassati, G. A. (2007). "Boundary Detailing of Coupled Core Wall System Wall Piers." *Journal of Advances in Structural Engineering* (under review).

Fortney P. J., Shahrooz B. M., and Rassati, G. A. (2007a). "Large Scale Testing of a Replaceable 'Fuse' Steel Coupling Beam." *Journal of Structural Engineering*, ASCE, 133(12), 1801-1807.

Fortney P. J., Shahrooz B. M., and Rassati, G. A. (2007b). "Seismic Performance Evaluation of Coupled Core Walls with Concrete and Steel Coupling Beams." *Journal of Steel and Composite Structures*, 7(4), 279-301.

Fortney P. J., Noe S., Rassati, G. A., and Shahrooz B. M., (2006). "A Steel-Concrete Composite Solution for Practical Design of Coupling Beams." in Mazzolani, F.M. and Wada, A., eds, *STESSA 2006: Behavior of Steel Structures in Seismic Areas*, pp 605-610, Taylor & Francis, London.

Fortney, P. J., (2005). "The Next Generation of Coupling Beams," Doctoral Dissertation, University of Cincinnati, Cincinnati, OH., pp.369.

Ghosh, S. and Markevicius, V., (1990). "Design of Earthquake Resistant Shearwalls to Prevent Shear Failure." *4th U.S. National Conference on Earthquake Engineering*, Earthquake Engineering Research Institute, Palm Springs. CA, Vol. 2, pp 905-913.

Gong B., Shahrooz B. M., and Gillum A. J. (1998), "Cyclic Response of Composite Coupling Beams." *ACI Special Publication 174 – Hybrid and Composite Structures*, ACI, Farmington Hills, Michigan: pp 89-112.

Gong B. and Shahrooz B. M. (2001a), "Steel-Concrete Composite Coupling Beams – Behavior and Design." *Engineering Structures*, 23(11), 1480-1490.

Gong B. and Shahrooz B. M. (2001b), "Concrete-Steel Composite Coupling Beams-Part I: Component Testing." *Journal of Structural Engineering*, ASCE, 127(6), 625-631.

Gong, B. and Shahrooz, B. M. (2001c), "Concrete-Steel Composite Coupling Beams-Part II: Subassembly Testing and Design Verification." *Journal of Structural Engineering*, ASCE, 127(6), 632-637.

Gong B., Shahrooz B. M., and Gillum A. J. (1998), "Cyclic response of composite coupling beams." *ACI Special Publication 174 – Hybrid and Composite Structures*, Farmington Hills, MI, pp 89-112.

Gupta, B., and Kunnath, S. K. (2000). "Adaptive spectra-based pushover procedure for seismic evaluation of structures." *Earthquake Spectra*, 16(2), 367-391.

Hajjar, J. F., Molodan, A., and Schiller, P. H. (1998). "A distributed plasticity model for cyclic analysis of concrete-filled steel tube beam-columns and composite frames." *Engineering Structures*, 20(4-6), 398-412.

Harries, K. A. (2001). "Ductility and Deformability of Coupling Beams in Reinforced Concrete Coupled Walls." *Earthquake Spectra*, 17(3), 457-478.

Harries, K. A., Fortney, P.J., Shahrooz, B. M. and Brienen, P., (2005). "Design of Practical Diagonally Reinforced Concrete Coupling Beams – A Critical Review of ACI 318 Requirements." *ACI Structures Journal*. 102(6), 876-882.

Harries, K. A., Gong, B., and Shahrooz, B. M. (2000), "Behavior and Design of Reinforced Concrete, Steel, and Steel-Concrete Coupling Beams." *Earthquake Spectra*, 16(4), 775-799.

Harries, K. A**.** and McNeice, D. S., (2006). "Performance-Based Design of High-Rise Coupled Wall Systems." *The Structural Design of Tall and Special Structures*, 15(3), 289-306.

Harries, K. A., Mitchell, D., Cook, W. D. and Redwood, R. G., (1992). "Seismic response of steel beams coupling reinforced concrete walls." *Journal of the Structural Division*, ASCE, 119(12), 3611-3629.

Harries, K. A., Mitchell, D., Redwood, R. G. and Cook, W. D. (1997). "Seismic Design of Coupling Beams - A Case for Mixed Construction." *Canadian Journal of Civil Engineering*, 24(3), 448-459.

Harries, K. A., Mitchell, D., Redwood, R. G., and Cook, W. D. (1998). "Nonlinear Seismic Response Predictions of Walls Coupled with Steel and Concrete Beams." *Canadian Journal of Civil Engineering*, 25(5), 803-818.

Harries, K. A., Mitchell, D., Cook, W. D., and Redwood, R. G. (1993). " Seismic Response of Steel Beams Coupling Concrete Walls." *Journal of Structural Engineering*, ASCE, 119(12), 3611-3629.

Harries, K. A., Moulton, D. and Clemson, R. (2004a). "Parametric Study of Coupled Wall Behavior – Implications for the Design of Coupling Beams." *Journal of Structural Engineering*, ASCE, 130(3), 480-488.

Harries, K. A., Shahrooz, B. M., Brienen, P. and Fortney, P. J. (2004b). "Performance Based Design of Coupled Walls." *Proceedings of the 5th International Conference on Composite Construction*, South Africa, July 2004.

Harries, K. A. and Shahrooz, B. M. (2005). "Hybrid Coupled Wall Systems – State of the Art." *Concrete International*, May 2005, pp. 45-51.

Hassan, M. and El-Tawil S. (2004), "Inelastic Dynamic Behavior of Hybrid Coupled Walls." *Journal of Structural Engineering*, ASCE, 130(2), 285-296.

Hassan, M. and El-Tawil, S. (2003), "Tension Flange Effective Width in Flanged RC Shear Walls." *ACI Structural Journal*, 100(3), 1-8.

Hilmy, S.I. and Abel, J.F. (1985). "A strain-hardening concentrated plasticity model for nonlinear dynamic analysis of steel buildings." *NUMETA85, Numerical Methods in Engineering, Theory and Applications*, Vol. 1, 303-314.

Hull, D. H. and Harries, K. A. 2008 (in press). "On the Applicability of Fixed Point Theory to the Behavior of Coupled Core Walls." *International Journal of Structural Stability and Dynamics*.

ICC (2003). International Building Code 2003, *International Code Council*, Falls Church, VA.

Imbsen Software Systems, (2004). *XTRACT – cross sectional X sTRuctural Analysis of ComponenTs*, v2.6.0. Computer Program.

Jan, T. S., Liu, M. W., and Kao, Y. C. (2003). "An upper-bound pushover analysis procedure for estimating the seismic demands of high-rise buildings." *Engineering Structures*, 26, 117-128.

Kabeyasawa, T., (1993). "Ultimate-State Design of Wall-Frame Structures." *Earthquake Resistance of Reinforced Concrete Structures*, A Volume Honoring Hiroyuki Aoyama," Editor: T. Okada, Department of Architecture, Faculty of Engineering, University of Tokyo, Japan, pp 431-440.

Kalkan, E. and Kunnath, S.K. (2006). "Adaptive Modal Combination Procedure for Nonlinear Static Analysis of Building Structures." *Journal of Structural Engineering*, ASCE, 132(11), 1721-1731.

Kanno, R. (1993). "Strength, Deformation, and Seismic Resistance of Joints between Steel Beams and Reinforced Concrete Columns." *Ph.D. Dissertation*, Cornell University, Ithaca, NY.

Kunnath, S. K., (2004). "Identification of modal combinations for nonlinear static analysis of building structures." *Computer-Aided Civil and Infrastructure Engineering*, 19, 282-295.

Kurama, Y., (2002)." Hybrid Post-Tensioned Precast Concrete Walls for Use in Seismic Regions." *PCI Journal*, Precast/Prestressed Concrete Institute, 47(5), 36-59.

Kurama, Y., Sause, R., Pessiki, S., and Lu, L.W., (2002). "Seismic Response Evaluation of Unbonded Post-Tensioned Precast Walls." *ACI Structural Journal*, 99(5), 641-651.

Kurama, Y. and Shen, Q., (2004). "Post-Tensioned Hybrid Coupled Walls Under Lateral Loads." *Journal of Structural Engineering*, ASCE, 130(2), 297-309.

Kurama, Y., Weldon, B., and Shen, Q., (2004). "Experimental Evaluation of Unbonded Post-Tensioned Hybrid Coupled Wall Subassemblages." *13th World Conference on Earthquake Engineering*, Vancouver, BC, Canada, August 1-6, 2004, 15 pp. (CD-ROM)

Kurama, Y., Weldon, B., and Shen, Q., (2006). "Experimental Evaluation of Post-Tensioned Hybrid Coupled Wall Subassemblages." *Journal of Structural Engineering*, ASCE, 132(7), 1017-1029.

Lehmkuhl, E. (2002). "Renaissance – A composite coupled shear wall system." *Proceedings of the 2002 SEAOC Convention* and additional personal correspondence.

Lim, A.K.W (1989). "The Nonlinear Response of Reinforced Concrete Coupling Slabs with Drop Panels in Earthquake Resisting Shearwall Structures.", M.Eng. Thesis, McGill University, pp 166.

Marcakis K. and Mitchell D. (1980). "Precast concrete connections with embedded steel members." *PCI Journal*, Prestressed/Precast Concrete Institute, 25 (4), 88-116.

Mattock A. H. and Gaafar G. H. (1982). "Strength of embedded steel sections as brackets." *ACI Structural Journal*, 79 (2).

Morgen, B. and Kurama, Y., "A Friction Damper for Post-Tensioned Precast Concrete Moment Frames." *PCI Journal*, Precast/Prestressed Concrete Institute, 49(9), 112-133.

Morgen, B. and Kurama, Y., "Friction-Damped Unbonded Post-Tensioned Precast Concrete Moment Frame Structures for Seismic Regions.," Structural Engineering Research Report #NDSE-07-01, Department of Civil Engineering and Geological Sciences, University of Notre Dame, Notre Dame, IN, March 2007.

New Zealand Standards Association (NZS) (1995), *NZS 3101:1995 Concrete Structures Standard.*

New Zealand Standards Association (NZS) (1992), NZS 4203:*1992 Code of Practice for General Structural Design and Design Loadings for Buildings*.

Otani, S., Teshigawara, M., Hayashi, M., Ishii, T., Kawabata, I., and Kani, N., (1994). "Earthquake Response Characteristics of Reinforced Concrete Structural Walls." *4th Meeting of the U.S.-Japan Joint Technical Coordinating Committee on Precast Seismic Structural Systems*, Tsukuba, Japan, May 1994.

Pantazopoulou, S. J. and Moehle J.P. (1990). "Identification of effect of Slabs on Flexural Behavior of Beams." *Journal of Structural Engineering*, ASCE, 116(1), 91-104.

Popov, E. P., Engelhardt, M. D. and Ricles, J. M. (1989). "Eccentrically Braced Frames: US Practice." *Engineering Journal*, AISC, 26(2), 66-80.

Paulay, T. and Santhakumar, A. R. (1976). "Ductile behavior of coupled shear walls." Journal of the Structural Division, ASCE, 102(ST1) 93-108.

Precast/Prestressed Concrete Institute (PCI) (1999). *PCI Design Handbook*, fifth edition.

Priestley, M. J. N. and MacRae, G. A. (1996). "Seismic Tests of Precast Beam-to-Column Joint Subassemblages with Unbonded Tendons." *PCI Journal*, Precast/Prestressed Concrete Institute, 41(1), 64-81.

Qin, F., (1993). Analysis of Composite Connection between Reinforced Concrete Walls and Steel Coupling Beams, M.S. Thesis, University of Cincinnati, Cincinnati, OH., 154

Rassati, G. A., Fortney, J. P., and Shahrooz, B. M. (2006). "Hybrid Coupled Core Wall Systems: An Innovative Approach to Post-Event Damage Mitigation." *Proc. of the Eighth U.S. National Conference on Earthquake Engineering*.

SEAOC (1999). "Structural Engineers Association of California (SEAOC) Blue Book: *Seismic* Design Recommendations of the SEAOC Seismology Committee." SEAOC, Sacramento CA.

Shahrooz B. M., Remmetter M. A. and Qin F. (1992). “Seismic Response of Composite Coupled Walls.” *Composite Construction in Steel and Concrete II*, ASCE, pp 429-441.

Shahrooz, B. M., Remetter, M. E., and Qin, F. (1993). "Seismic Design and Performance of Composite Coupled Walls." *Journal of Structural Engineering*, ASCE, 119(11), 3291-3309.

Shahrooz B. M., Deason J. T., and Tunc G. (2004a). “Outrigger Beam – Wall Connections: Part I-Component Testing and Development of Design Model.” *Journal of Structural Engineering*, ASCE, 30(2):253-261.

Shahrooz B. M., Tunc G., and Deason J. T. (2004b). “Outrigger Beam – Wall Connections: Part II-Subassembly Testing and Further Modeling Enhancements.” *Journal of Structural Engineering*, ASCE, 130(2), 262-270.

Shahrooz B. M., Gong B., Tunc G. , and Deason J. D. (2001). “An Overview of Reinforced Concrete Core Wall-Steel Frame Hybrid Structures.” *Progress in Structural Engineering and Materials*, 3(2): 149-158.

Shen, Q. and Kurama, Y., (2002). “Nonlinear Behavior of Posttensioned Hybrid Coupled Wall Subassemblages.” *Journal of Structural Engineering*, ASCE, 128(10), 1290-1300.

Shen, Q., Kurama, Y., and Weldon, B., (2006a). “Seismic Design and Analytical Modeling of Post-Tensioned Hybrid Coupled Wall Subassemblages.” *Journal of Structural Engineering*, ASCE, 132(7), 1030-1040.

Shen, Q., Kurama, Y., and Weldon, B., (2006b). “Seismic Analysis, Behavior, and Design of Unbonded Post-Tensioned Hybrid Coupled Wall Structures.” Structural Engineering Research Report #NDSE-06-02, Department of Civil Engineering and Geological Sciences, University of Notre Dame, Notre Dame, IN, December 2006b.

Spacone, E. and El-Tawil, S. (2004). “State-of-the-Art in Nonlinear Analysis of Composite Systems.” *Journal of Structural Engineering*, ASCE, 130(2), 159-168.

Subedi, N. K., (1989). “Reinforced concrete beams with plate reinforcement for shear.” Proc. *Instn. Civ. Engrs.*, Part 2 (87), 377-399.

Takeda, T., Sozen, M.A., and Nielsen, N. (1970). “Reinforced concrete response to simulated earthquakes.” *Journal of Structural Engineering*, ASCE, 96(12), 2557-2573.

Taranath, B.S. (1998). *Steel, Concrete and Composite Design of Tall Buildings*, 2nd edition. McGraw Hill, New York. pp 998.

Xuan, G. and Shahrooz B. M. (2005). "Performance Based Design of a 15 Story Reinforced Concrete Coupled Core Wall Structure." Report No. UC-CII 05/03, Cincinnati Infrastructure Institute.

Xuan G., Shahrooz B.M., Harries K.A., Rassati G.A., (2008). "A Performance-Based Design Approach for Coupled Core Wall Systems with Diagonally Reinforced Concrete Coupling Beams." *Advances in Structural Engineering*, 11(3), 265-280.

Index